Journal of Structural Geology 140 (2020) 104157

Contents lists available at ScienceDirect

Journal of Structural Geology

journal homepage: http://www.elsevier.com/locate/jsg

Evaluation of the Plio-Quaternary tectonic stress regime from fault kinematic analysis in the lake Van Basin (Eastern Anatolia)

Azad Sağlam Selçuk [a,*], Mehmet Korhan Erturaç [b,c], Gürsel Sunal [d], Ziyadin Çakır [d]

[a] Yüzüncü Yıl University, Department of Geological Engineering, TR-65100 Van, Turkey
[b] Sakarya University, Department of Geography, Sakarya, Turkey
[c] Sakarya University, Research Development and Application Center (SARGEM), Esentepe Campus, 54187, Sakarya, Turkey
[d] Istanbul Technical University, Department of Geology, Ayazağa/Istanbul, Turkey

ARTICLE INFO

Keywords:
Lake Van basin
East Anatolia
Kinematic analysis
Transpression
Stress regime, Pleistocene lake terraces

ABSTRACT

We focus on the Neogene–Quaternary tectonic evolution of the Lake Van Basin located within the Turkish-Iranian Plateau. To better understand the complex tectonic history of the region and determine the paleo-stress patterns, we investigate and report on the geometric, structural, and kinematic characteristics of the Basin based on field observations of fault-slip orientations which are classified according to radiometric ages of the basin stratigraphy.

The analysis of large-scale structures and fault kinematics indicate that three different deformation phases prevailed in the Lake Van Basin during the Neogene-Quaternary periods. Phase 1 is characterized by NW-SE extension and NE-SW contraction that gave rise to the development of strike-slip faults with thrust or normal components during the late Miocene, deforming the fluvial sediments which expose at east/northeast of the Basin. Phase 2 is characterized in fluvial and lake deposits of the Middle Pleistocene, deformed by dominant contraction stress regime effective along NW-SE direction. The late Pleistocene tectonic regime (Phase 3) consists of transpressional deformation that develops under NNW-SSE compression and ENE-WSW extension. According to our analysis, the present-day deformation pattern of the Lake Van Basin is dominated by compression at east, while at the northern part is transtensional.

1. Introduction

Eastern Anatolia has been widely studied over the last decades because it is one of the rare places where you can investigate tectonic processes take affect due to the collision of two continental plates (Arabia and Eurasia) within a very narrow zone (Fig. 1a). As a result of the ongoing collision, there are frequent devastating earthquakes associated with strike and reverse slip faults, active volcanism, metamorphic zones bearing the first traces of this collision, and Miocene-Quaternary deposits. Additionaly, numerious seismogenic faults have been identified throughout eastern Anatolia (Arpat et al., 1977; Şaroğlu et al., 1984; Şaroğlu and Yılmaz, 1986; Şaroğlu et al., 1987; Cisternas et al., 1989; Rebai et al., 1993; Koçyiğit et al., 2001; Dhont and Chorowicz, 2006; Horasan and Boztepe-Güney, 2007; Sağlam-Selçuk et al., 2016; Gürbüz and Şaroğlu, 2019).

Eastern Anatolia encompasses the East Anatolian High Plateau (EAHP) (Şengör and Kidd, 1979; Şengör and Yılmaz, 1983). The Plateau formed about 13 Ma years ago due to the continent-continent collision of Arabia with Eurasia (Şengör and Kidd, 1979; Şengör and Yılmaz, 1983; Dewey et al., 1986; Şaroğlu and Yılmaz, 1986; Yilmaz et al., 1987; Koçyiğit et al., 2001). The EAHP is currently experiencing nearly N–S motion with respect to Eurasia at a rate of 13–15 mm/year, and E-W continental extension (Şengör and Yılmaz, 1983; Koçyiğit et al., 2001; Reilinger et al., 2006). This collision zone is bounded by Bitlis-Zagros fold-and-thrust belt to the south, the East Anatolian fault to the west, and Pembak–Sevan–Sunik Fault to the north. In the east, block modelling based on GPS data (Reilinger et al., 2006; Djamour et al., 2011) suggests two broad tectonic blocks (Caucasus and Turkish-Iran) that accommodate intracontinental deformation between the Arabian and Eurasian plates (Fig. 1b).

The Lake Van Basin (LVB) contains important records in the geodynamic structure of the EAHP (Fig. 1a–b). Şengör and Kidd (1979); Dewey et al. (1986); Şaroğlu and Yılmaz, 1986 suggest that the LVB is a product of the collision of the Arabian Plate with the Eurasia. The

* Corresponding author.
E-mail address: azadsaglam@yyu.edu.tr (A.S. Selçuk).

https://doi.org/10.1016/j.jsg.2020.104157
Received 17 January 2020; Received in revised form 20 July 2020; Accepted 6 August 2020
Available online 16 August 2020

formation of the LVB commenced in late Pliocene, and has taken its present shape with the influence of Quaternary volcanism (Blumenthal et al., 1964; Wong and Finckh, 1978; Degens et al., 1984).

Active faults in the LVB were mapped during recent field studies on land areas by Emre et al. (2013a) and Koçyiğit (2013). Detailed seismic investigations were also carried out recently in the lake (PaleoVan Project, Litt et al., 2009; Çukur et al., 2014; Özalp et al., 2016) (Fig. 1c). The analytical information on the kinematic characteristics of the faults in the region are only known from focal mechanism solutions of a few important instrumental earthquakes (PaleoVan Project, Litt et al., 2009; Çukur et al., 2014; Özalp et al., 2016) (Fig. 1c).

The lack of a distributed fault kinematic data for the LVB makes it difficult to determine the evolution of the tectonic regime in affect for the evolution of the region. The traces of tectonic development of the LVB are observed on the fault planes that cut volcanic and sedimentary rocks cropping out around the Lake. The fault slip data collected from the fault planes are temporally classified within the basin stratigraphy. The purpose of this study was to collect observations of fault kinematics from the rock groups of different lithologies and ages and to evaluate them by using graphical and computational kinematic analysis methods.

2. Geological and tectonic settings

2.1. The East Anatolian High Plateau (EAHP)

The East Anatolian High Plateau, and northwestern Iran and the Caucasus regions together form one of the broad zones of high elevation (average ~2 km) along the Alpine-Himalayan Mountain belt (Şengör and Yılmaz, 1983; Jackson, 1992; Şengör et al., 2003). The formation of the EAHP commenced following the northward subduction and the

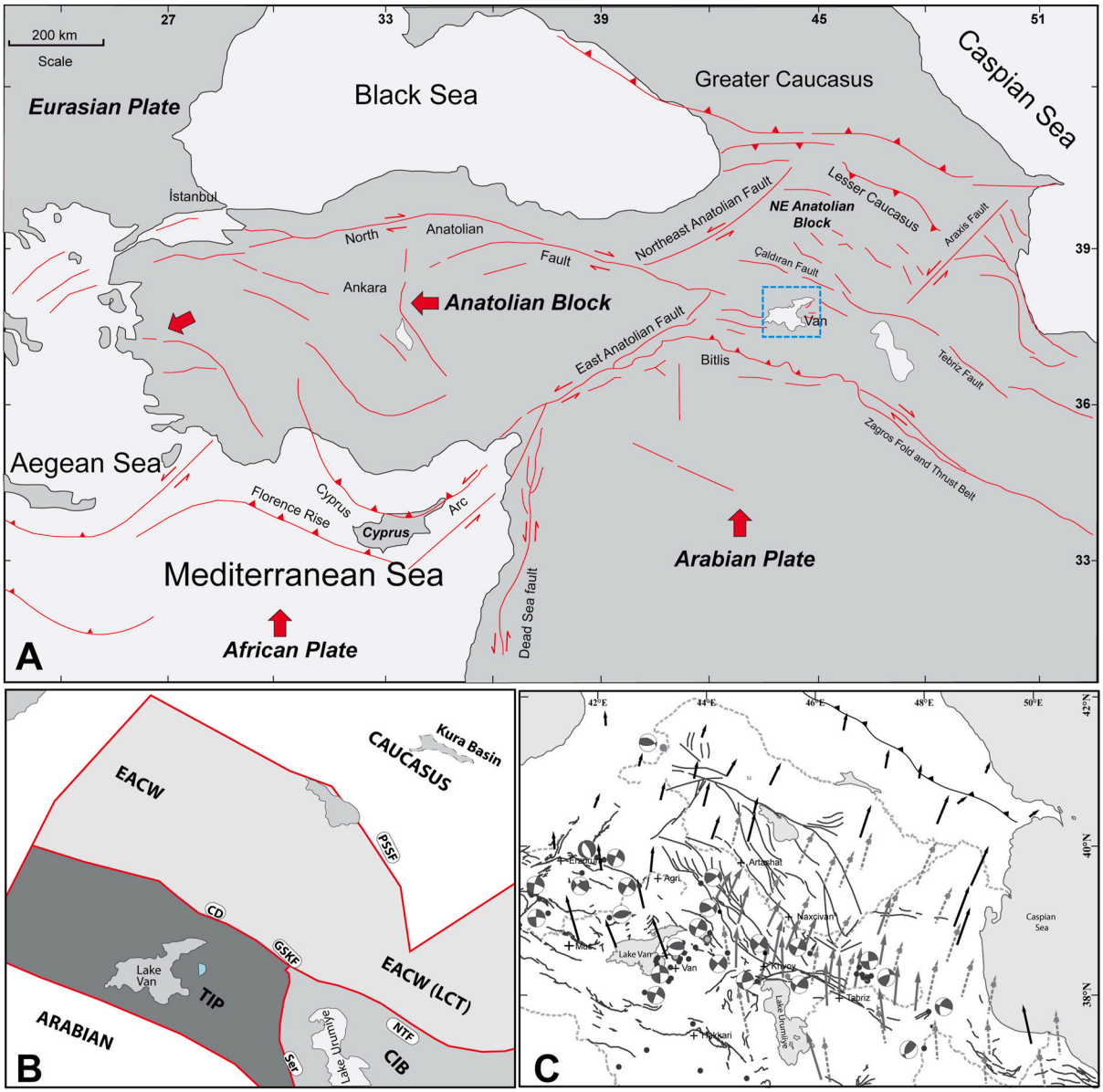

Fig. 1. a) Tectonic setting of the Eastern Mediterranean and the Middle East. The faults were compiled from various sources (Philip et al., 2001; Karakhanian et al., 2004; Hessami et al., 2003; Emre et al., 2013a), b) The tectonic blocks and slip rates are taken from McClusky et al., 2000; Reilinger et al. (2006) and Djamour et al. (2011). CD (Çaldıran Fault); EAHP (East Anatolian High Plateau); NTF (North Tabriz Fault); TIP (Turkish-Iranian Plateau), c) Active faults, seismicity and kinematics of the East Anatolian and Iranian High Plateau. Seismicity is from the USGS. The black circle indicates the locations of the moderate to large earthquakes. The focal mechanisms are from: McKenzie (1972); Toksoz et al. (1978); Taymaz (1990); Tan (2004), Tan et al. (2008); and CMT catalogue. GPS velocity vectors were compiled from Reilinger et al. (2006); Djamour et al. (2011) and Karakhanian et al. (2013).

closure of the Neotethyan oceanic gateway between the Mediterranean and the Indian Ocean during the Middle Miocene, and has been linked to extension of the Aegean, rifting of the Red Sea, and the formation of the North and East Anatolian fault systems (e.g., Jolivet and Faccenna, 2000). The collusion first led to crustal thickening of the Eurasian plate (Dewey et al., 1986) and then to extensive magmatism on both the Eurasian and Arabian plates (Pearce et al., 1990; Notsu et al., 1995; Ekici et al., 2007). The initiation of intracontinental deformation and the associated tectonic activity is evidenced by apatite fission track dating of the exhumation of the Bitlis-Zagros thrust belt 18-13 Ma ago (Okay et al., 2010). Today, the convergence continues at a rate of approximately 15 mm/yr based on GPS observations (Reilinger et al., 2006) (Fig. 1c). Deformation within the EAHP is partitioned into a NW-SE oriented, subparallel series of dextral strike-slip faults, and thrust faulting (Jackson, 1992). The right-lateral strike-slip faulting north of the EAHP accommodates the motion between the counter-clockwise rotating crustal blocks and also increases the shortening rate along the Caucasus Range to the east (Reilinger et al., 2006; Copley and Jackson, 2006).

Over the past few decades, pivotal studies of the post collisional evolution, and the geodynamic properties of the region, have been advanced with the help of new data such as upper mantle P-wave tomographic modeling foreastern Turkey and surrounding regions (Zor et al., 2003; Zor, 2008), providing new constraints on the evolution of the Eastern Anatolian crust since early Miocene (Gök et al., 2003; Şengör et al., 2003; Zor et al., 2003; Faccenna et al., 2006; Zor, 2008). These studies documented that the mantle lithosphere is either very thin or absent beneath a considerable portion of the EAHP (Türkelli et al., 1996; Sandvol et al., 1998; Gök et al., 2000; Al-Lazki et al., 2003; Zor et al., 2003; Angus et al., 2006; Özacar et al., 2008, 2010). It is widely accepted that the domal uplift of the EAHP is associated with the steepening and break-off of the northward subducting Arabian lithosphere (~11 Ma). Keskin et al. (1998) and Şengör et al. (2003) proposed that the upwelling of hot asthenosphere caused the recent widespread volcanism in the EAHP, that displays different eruption styles (from shield to stratovolcanoes and also monogenic volcano fields and domes) and chemical characteristics (from alkaline to calc-alkaline) (Innocenti et al., 1976, 1980; Pearce et al., 1990; Keskin et al., 1998; Lebedev et al., 2010). Consequently, the mechanical behavior of the very thin crust gave rise to variations in the stress field (Şengör et al., 2003), forming distributed faults, and giving the appearance of relatively small tectonic blocks. Within this deformation field, the dominant, active structures are NW-SE striking dextral, and NE-SW striking sinistral strike-slip faults, which accommodate 70% of the deformation (Reilinger et al., 2006). These faults are aligned subparallel, are very closely spaced, have relatively short lengths, and are dispersed from south of the Lake Van towards the Caucasus Range (Fig. 1c). They have distinct surface expressions and have caused devastating historical and instrumemtally recorded earthquakes (Fig. 1c). Several studies with details have been published on the geometry, kinematics, age, and geological slip rates of these faults (Toksöz et al., 1977; Şaroğlu, 1986; Şaroğlu and Yılmaz, 1986; Barka and Kadinsky-Cade, 1988; Şaroğlu et al., 1992; Jackson, 1992; Trifonov et al., 1996; Bozkurt, 2001; Koçyiğit et al., 2001; Philip et al., 2001; Hessami et al., 2003; Karakhanian et al., 2004; Dhont et al., 2006; Solaymani Azad et al., 2015; Selçuk et al., 2010; Emre et al., 2013b; Rizza et al., 2013). The overall tectonic framework of the region was reviewed by Jackson (1992) and Copley and Jackson (2006).

The seismicity of the region is distributed discontinuously along these faults. Although most faults caused moderate to large earthquakes during the 20th century, more devastating events were reported for the historical period (see reviews by Ambraseys, 2009 and Berberian, 2014). The active faults of Armenia and Iran have been studied extensively by means of paleoseismology (Philip et al., 2001; Hessami et al., 2003; Karakhanian et al., 2004; Solaymani Azad et al., 2015). However, detailed investigations (mapping and paleoseismological studies) of the active faults from East Anatolia are still in progress because recognition of some of the main faults was only possible after their recent seismic activity (e.g. 2011 Van Earthquake, Mw = 7.1, Elliot et al., 2013).

Recent kinematic block models using data from the increasing number of GPS observations(e.g., Djamour et al., 2011, Khorrami et al., 2019) describe the Lesser Caucasus-Talesh (LCT) block, the Turkish-Iranian Plateau (TIP) block, and the Central Iranian Block (CIB) within these blocks (Fig. 1b). However, numerous smaller fault systems influence the internal deformation within these blocks forming boundaries of smaller blocks (e.g., Copley and Jackson, 2006). Karakhanian et al. (2013) further divided these blocks into smaller ones attributing each block bounding fault an annual slip rate close to the measurement errors using data from a denser GPS network in Armenia (Fig. 1c).

2.2. The Lake Van Basin (LVB)

The Lake Van Basin (LVB) is bounded in the west by Nemrut volcano, in the south by the Bitlis-Zagros Structure Zone, in the east by the Serevan Fault, and in the north by the Çaldıran Fault. The LVB is one of the products of the continent-continent collision that started as a result of the oceanic closure by the subduction of the Arabian Plate beneath the Eurasian Plate (Şengör and Kidd, 1979; Dewey et al., 1986; Şaroğlu and Yılmaz, 1986). The LVB began to develop in late Pliocene and developed its present structure in association with the volcanism that initiated in the Quaternary (Blumenthal et al., 1964; Wong and Finckh, 1978; Degens et al., 1984). N–S compressional tectonic regime has been dominated with collision in this region. Koçyiğit et al. (2001) suggests that the compressional tectonic regime was only effective along the Bitlis-Zagros suture zone between the late Miocene and early Pliocene. During this tectonic regime, NW-NE striking strike slip faults, E-W striking reverse/thrust faults and folds, and N–S striking normal faults and tensional fissures, developed in the region (Arpat et al., 1977; Şaroğlu et al., 1987; Cisternas et al., 1989; Koçyiğit et al., 2001; Dhont and Chorowicz, 2006; Doğan and Karakaş, 2013; Sağlam-Selçuk et al., 2016; Akoğlu et al., 2018; Akkaya and Özvan, 2019). Major neotectonic structures are shown in Fig. 2.

Recent studies in the region have shown that Lake Van is thought to have formed ~600,000 years ago (Stockhecke et al., 2014a; Çukur et al., 2014) and is the largest sodic lake in the world, with a surface area of 3570 km^2, volume of 607 km^3, and maximum depth of 451 m (Kempe et al., 1978). Since its formation, the water level of the Lake has shown significant variations until today. The highest water level of Van Lake, which today stands at 1650 m above sea level, has been estimated to be maximum 1720 m (±70 m) by Degens et al. (1978) and 1755 m (±108 m) by Kuzucuoğlu et al. (2010) and Görür et al. (2015), and 1705m (±55m) by Kuzucuoğlu et al. (2010), Çağatay et al. (2014) and Görür et al. (2015). Lake deposits, which formed as a result of these water level changes and tectonic and climatic factors (the Lake Van formation), are widespread, particularly to the east of the Lake (Aksoy, 1988; Acarlar et al., 1991; Üner et al., 2010; Kuzucuoğlu et al., 2010).

The major active faults in LVB have led to the occurrence of earthquakes of different magnitudes during the historical and instrumental period. According to historical earthquake records, the LVB was affected by 13 earthquakes with intensities of V-X between at 1101 and 1900 (Ergin et al., 1967; Soysal et al., 1981; Ambraseys ve Finkel, 2006; Tan et al., 2008), casusing destruction in the region in the 1101, 1894 and 1900, Vaspaskuran (Van) earthquakes. One of the most important Van earthquakes occurred in the early 17th century with aftershocks continuing for more than 3 years (Ambraseys, 2009). The earthquakes that occurred west of the LVB are thought to be related to the volcanic activity in the vicinity of the Nemrut Caldera (Ambraseys ve Finkel, 1995). However, these earthquakes are known to affect the province of Van. In addition, VI-VIII intensity earthquakes occurred in Xosap (Hoşap), southeast of Van, in the 16th and 17th centuries (Ergin et al., 1967; Soysal et al., 1981; Ambraseys and Finkel, 2006; Tan et al., 2008). These earthquakes caused damage from Van to Ercis cities. An earthquake in 1648 destroyed villages in a large area where many big

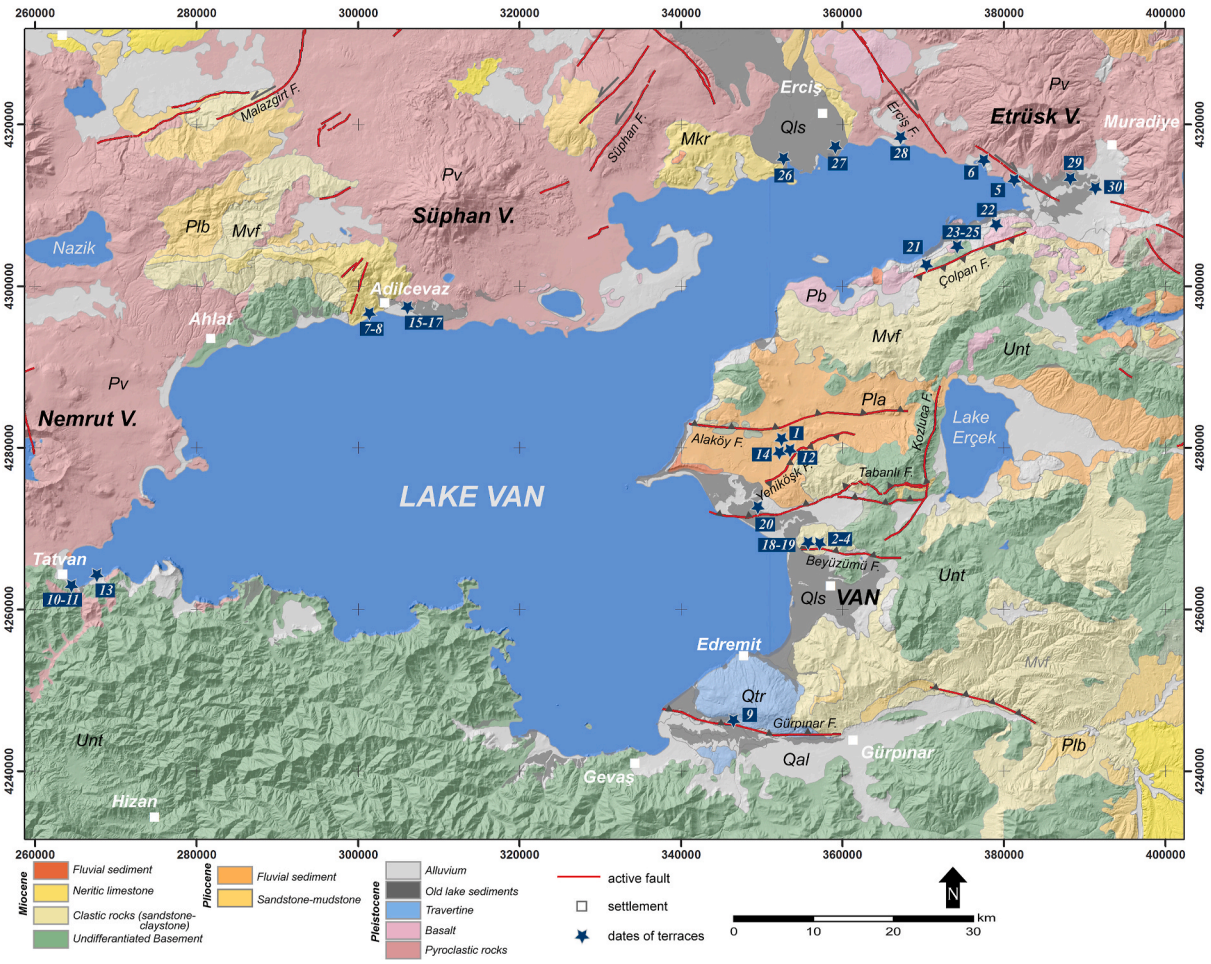

Fig. 2. The geology of the Lake Van Basin (the geology was modified from Ateş et al., 2007 and active faults were modified from Emre et al., 2013a). Numbers indicate the absolute age determinations of ancient terraces of the Van Lake (Table 1).

landslides occurred and the aftershocks lasted for more than three months (Ambraseys and Finkel, 1995; Ambraseys, 2009).

During the instrumental period, 95 earthquakes with magnitudes greater than 4.0 were recorded in the LVB (KOERİ, 2020). Of these, the Çaldıran earthquake (Mw 7.3) and Van earthquake (Mw 7.2) were the two most devastating. The Çaldıran fault that bounds the LVB to the north (Sağlam-Selçuk et al., 2016), produced the Mw 7.3 1976 Çaldıran event, causing nearly 5000 deaths, and destruction of more than 10,000 houses in the region (Arpat et al., 1977). The focal mechanism solution of the earthquake indicate pure dextral strike-slip motion. The 23 October 2011 (13:41, GMT+2) Mw 7.2 Van earthquake occurred east of Lake Van. The earthquake caused a loss of >600 lives and extensive damage to more than 10,000 of houses. The aftershocks continued for two years, with >6000 aftershocks recorded. The focal mechanism solution of the mainshock revealed thrust faulting.

The focal mechanism solutions for recent earthquakes (1988, 1999, 2000, 2001, 2003, 2011 earthquakes) indicate that earthquakes in the eastern part of the LVB prominently have reverse faulting mechanisms (REDPUMA, 2003; KOERİ, 2011; EMSC, 2011; USGS, 2011; TÜBİTAK, 2011). Focal mechanism solutions west and north of the Basin indicate strike-slip faulting (REDPUMA, 2003; KOERİ, 2011; EMSC, 2011; USGS, 2011; TÜBİTAK, 2011), defining a stress regime where the principal stress component (σ_1) NNW-SSE, and with the vertical intermediate stress component (σ_2) (Toksöz et al., 1983; Cisternas et al., 1989; Ambraseys and Jackson, 1998; Ambraseys, 2001; Tan et al., 2008; KOERI, 2011).

2.3. Geology and stratigraphy of the LVB

The LVB has a heterogenous stratigraphical basement that crops out along the circumferences of the lake. Geological formations on the northern and western parts of the lake, are mainly Neogene and Quaternary volcanic rocks, and in some places clastic and carbonate Miocene sediments (Fig. 2). The Upper Cretaceous-Oligocene ophiolitic mélange and flyschoidal units, which constitute the East Anatolian Accrettionary Complex, are observed mostly on the eastern margin (Üner, 2019; Mutlu and Üner, 2019). The southern margin is generally represented by the Paleozoic metamorphic rocks of the Bitlis Massif. All these rocks form the source areas of 700 m thick sediments that have accumulated in the Lake since its formation 600 thousands yearsago (Litt et al., 2009; Stockhecke et al., 2014a, b; Çukur et al., 2014). On the southern, eastern, and northern the Lake Van Basin, old fluvial sediments, basalts, terrace deposits of the Lake Van, and young river deposits are widely distributed (Fig. 2).

The old terrigenous sedimentary units are formed by the alternation of sandstones, siltstones and conglomerates of the Kurtdeliği formation. These units are unconformably overlain by sandstone and pumice within the basalt flow and the Lake Van terrace deposits (Fig. 3). The succession is generally formed of badly sorted, medium to thick-layered, reddish polygenic, and sometimes monogenic, pebbly conglomerate layers. It is well compacted and cemented with calcite. The old terrestrial deposits possess a significant position within the young sedimentary stratigraphy because they are stratigraphically located between the Miocene Van Formation (the latest turbiditic sediments deposited in the Paleotectonic

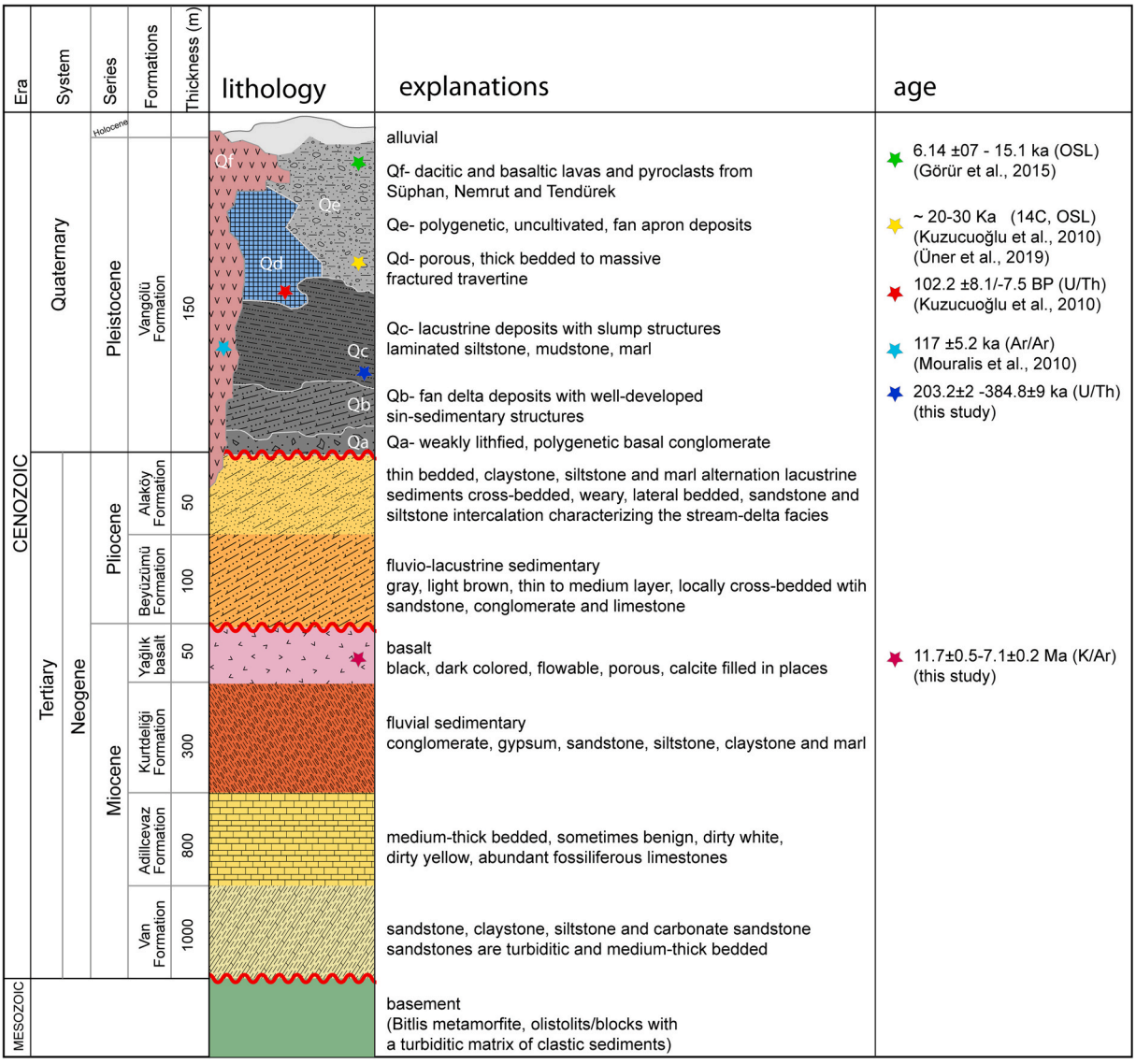

Fig. 3. The generalized stratigraphical section of the Lake Van Basin (modified from Ateş et al., 2007).

period) and the Pliocene units. In addition, the absence of clastics of volcanic origin indicates that they precede the onset of the widespread volcanism in the region. Based on their stratigraphic position, these deposits are regarded as late Miocene in age.

Basalts are generally dark brown to black with large pores and have flow structures. However, there are widely observed baked zones in lower parts of them. Around the Ermişler village, the basalt unconformably overlies the old terrestrial sediments (Fig. 3). In interlayers of these basaltic flows, there are some pumice levels that have internal structures probably due to the stagnant lake environment, and derived from volcanics. Basalt samples were taken from three different locations around Ermişler village (northeast of Lake Van). Samples were dated by the K/Ar dating (Isotope Laboratory IGEM RAS, V.A. Lebedev), providing ages of 18.8 ± 1 Ma, 11.7 ± 0.5 Ma and 7.1 ± 0.2 Ma (Table 1). Innocenti et al. (1976) reported ages of 3.9 (±0.1) Ma with K/Ar method from basalts located southeast of Muradiye County. It was pointed out that the same age has been reported for the basalts located northeast of Lake Van (Acarlar et al., 1991).

East of the Lake Van Basin, there are former lake deposits (terraces) that consist of sandstone, claystone and conglomerates, exposing in a wide area. These terrace deposits reach to an elevation of 1750 m and were defined as the uppermost terrace level of the Basin (the Beyüzümü terrace) by Kuzucuoğlu et al. (2010) (Table 1-Fig. 4). Sandstones are well leached, loosely compacted, yellow to gray colored, fine- to medium-grained, and seldom cross-bedded. Cross-beddings are cut by tiny channel fillings. The grain size varies between fine to coarse, and fine sandstones are bioturbated. Fossilliferous layers with abundant *Dreissensia* sp. alternating with sandstones become dense towards the upper layers of the unit. Again, towards the upper layers of the deposit, the conglomerate layers alternating with sandstone are remarkable. Pebbles are well sorted and loosely compacted with a sandy matrix.

The alluvial fan and fluvial deposits exhibit an extensive distribution in the LVB. Fan deposits are formed by pebble, sand, and mud. Delta sediments are made up of fine-grained material, whereas the fan delta deposits are formed by sandy, silty, and pebbly layers. These units are Quaternary in age, and deformed in the areas closer to the fault zones. However, they do not present any evidence of deformation at a certain distance from the fault zones.

Terrace levels are exposed at elevations varying between 1656 and 1800 m around the Lake (Figs. 2 and 3). These deposits have well-preserved, sedimentary structures, with thicknesses varying from 3 to 25 m, and belong to offshore and the lakeside, providing significant information about their depositional environment (Görür et al., 2015). Dating was performed by means of radiocarbon, OSL, and $^{234}Th/^{238}U$

Table 1
The ages of terraces around the Lake Van. The compiled data are from Kempe et al. (2002), Kuzuoğlu et al. (2010), Mouralis et al. (2010), Görür et al. (2015), Üner et al. (2019) and this study.

Site	No	Name	LON (°E)	LAT (°N)	Age	Horizon	Material	Method	Reference
Yumrutepe (YUM 4)	1	Van 05-49	43,311	38,673	>34000 BP	Shells at beach level	$CaCO_3$	Radiocarbon	Kuzucuoğlu et al. (2010)
Beyüzümü	2	Van 05-51	43,392	38,537	>31000 BP	Shells on top layer (above peat)	$CaCO_3$	Radiocarbon	Kuzucuoğlu et al. (2010)
Beyüzümü	3	Van 06-BT 10-15	43,392	38,537	>34000 BP	Top of 2.5 m peat sequence	Organic	Radiocarbon	Kuzucuoğlu et al. (2010)
Beyüzümü	4	Van 06-01	43,392	38,537	>30000 BP	Peat Layer 7b within (top) sequence	Organic	Radiocarbon	Kuzucuoğlu et al. (2010)
Kırklar	5	Van 05–36b	43,607	38,968	24900 ± 800cal. BP	Black layer below tephra (sup.)	Organic	Radiocarbon	Kuzucuoğlu et al. (2010)
Kırklar	6	Van 05-36a	43,580	38,982	25700 ± 600cal. BP	Black layer below tephra (inc.)	Organic	Radiocarbon	Kuzucuoğlu et al. (2010)
Adilcevaz	7	Van 06-76a	42,748	38,806	5940–6185cal. BP	Charcoal associated with ceramics	Charcoal	Radiocarbon	Kuzucuoğlu et al. (2010)
Adilcevaz	8	Van 06–76b	42,753	38,806	9470–9550cal. BP	Charcoal in aceramic layers (base)	Charcoal	Radiocarbon	Kuzucuoğlu et al. (2010)
Güzeldere (Apricots)	9		43,220	38,336	20700 ± 300cal. BP	Organic matter (upper level)	Organic	Radiocarbon	Kempe et al. (2002)
Kotum	10	06-33 sup.	42.309	38.472	102.2 + 3.8/-3.7 BP	Low travertine		U/Th	Kuzucuoğlu et al. (2010)
Kotum	11	06-33 inf.	42.309	38.472	102.1 + 8.1/-7.5 BP	Low travertine		U/Th	Kuzucuoğlu et al. (2010)
Yumrutepe	12	OSL16	43.311	38.673	12 ± 1.8 ka	Nearshore lake sediments (?)	Polymineral	OSL	Görür et al. (2015)
Kotum-Küçüksu Valley	13	VAN 021	42,314	38,478	117 ± 5.2 ka	Pyroclastics (pumice fall)	Mineral	Ar/Ar	Mouralis et al. (2010)
Yumrutepe	14	OSL48-1	43.3102	38.674	10 ± 1 ka (n = 9),15 ± 1 ka(n = 25), 20±1ka (n = 9)	Nearshore lake sediments (?)	Quartz	OSL	Görür et al. (2015)
Adilcevaz	15	OSL27-1	42.757	38.805	10.3 ± 1.1 ka	Nearshore lake sediments (lower level)	Polymineral	OSL	Görür et al. (2015)
Adilcevaz	16	OSL27-2	42.757	38.805	6.14 ± 0.7 ka	Nearshore lake sediments (middle level)	Polymineral	OSL	Görür et al. (2015)
Adilcevaz	17	OSL27-3	42.757	38.805	8.2 ± 0.92 ka	Nearshore lake sediments (upperlevel)	Polymineral	OSL	Görür et al. (2015)
Beyüzümü	18	OSL54	43.391	38.537	15 ± 1 ka	Nearshore lake sediments	Quartz	OSL	Görür et al. (2015)
Çatakdibi	26	CTK-1	43.302	39.039	28.0 ± 2.8 33.1 ± 2.7 ka	Nearshore lake sediments (seismites)	Polymineral	OSL	Üner et al. (2019)
Haydarbey	27	HAY-1	43.431	39.010	23.2 ± 1.5 ka	Nearshore lake sediments (seismites)	Polymineral	OSL	Üner et al. (2019)
Erçiş	28	ERC1-5	43.358	39.029	24.2 ± 1.9 30.1 ± 1.8 ka	Nearshore lake sediments (seismites)	Polymineral	OSL	Üner et al. (2019)
Muradiye	29	MUR1-2	43.745	38.974	20.4 ± 1.6 27.9 ± 1.6 ka	Nearshore lake sediments (seismites)	Polymineral	OSL	Üner et al. (2019)
Beyüzümü	19	Byz-18	43.385	38.544	203 ± 2 ka	Shells at beach level	$CaCO_3$	U/Th	This study
Yeniköşk	20	Ynk-20b	43.293	38.605	267 ± 7 ka	Shells at beach level	$CaCO_3$	U/Th	This study
Gedikbulak	21	Gdk-22	43.384	38.841	214 ± 2 ka	Shells at beach level	CaCO3	U/Th	This study
Ermişler	22	Erm-33	43.592	38.917	384 ± 9 ka	Shells at beach level	CaCO3	U/Th	This study
Ermişler	23	Erm-24	43.515	38.872	11.7 ± 0.5 Ma	Basalt	Mineral	K/Ar	This study
Ermişler	24	Erm-24a	43.507	38.869	18.8 ± 1 Ma	Basalt	Mineral	K/Ar	This study
Ermişler	25	Erm-27	43.509	38.871	7.1 ± 0.2 Ma	Basalt	Mineral	K/Ar	This study

methods in previous investigations (Kempe et al., 2002; Kuzucuoğlu et al., 2010; Çağatay et al., 2014; Görür et al., 2015; Kamar, 2018; Üner et al., 2019), and by using the $^{234}Th/^{238}U$ method in this study (Table 1, Fig. 2). At six different locations east of Van Lake, *Dressencia* sp. shells were collected from levels of the lake terraces (Fig. 2). These shells were sent to the GEOTOP Laboratory in Canada for dating using the U/Th method. Here we report the oldest age from the Lake Van terraces, determined as 384.7 ± 9.1 ka from Çolpan, whereas another terrace step in the east (Beyüzümü) were also dated to 203.1 ± 2 ka (Table 1).

2.4. Active faults in the LVB

Studies performed on the active tectonics of the LVB became more detailed following the 2011 earthquake. A major focuse of these studies is the basic characteristics of the main fault that had produced the earthquake (Özkaymak et al., 2011; Bayraktar et al., 2013; Görgün, 2013; Doğan and Karakaş, 2013; Altıner et al., 2013; Elliott et al., 2013; Akoğlu et al., 2018). The General Directorate of Mineral and Exploration (MTA) carried out a mapping study for all active faults in Turkey (Emre et al., 2013a,b), including the classification of the faults based on their activity periods (e.g. Holocene fault, Quaternary fault, Earthquake surface break and etc.) (Fig. 4). During the production of this map, detailed field surveys were carried out focusing the active faults in the LVB (Beyüzümü Fault (BF), Van/Everek Fault (VFZ), Yeni Köşk Fault (YF), Çolpan Fault (Caf), Kozluca Fault and Erçiş Fault (EF) (Fig. 4).

2.4.1. The Beyüzümü Fault

The Beyüzümü Fault is a nearly 20 km-long thrust fault (Fig. 5a–b) starting from the Kalecik village located north of the Van City center to the north of the Sıhke Lake (Mackenzie et al., 2016) (Fig. 4). It was first

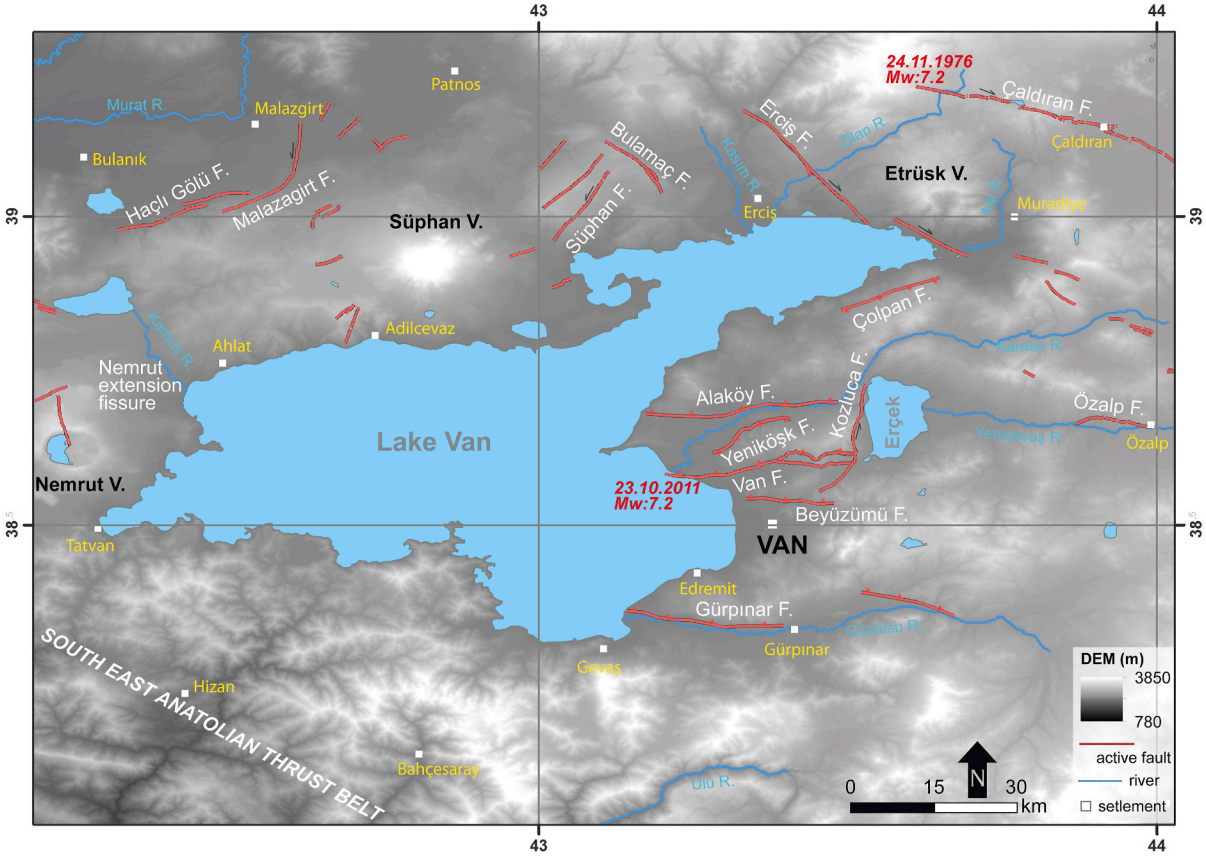

Fig. 4. Maps of the simplified active faults of the Lake Van Basin (faults from: Koçyiğit, 2013; Emre et al., 2013a; Doğan ve Karakaş, 2013; Sağlam Selçuk et al., 2016).

identified by Lahn (1946), and then named the "Beyüzümü Fault" by Ateş et al. (2007), and the "Kalecik Fault" by Koçyiğit (2013). In June and December of 1945, two earthquakes happened that affected the center and districts of the Van City with magnitude of 5.8 (M). National newspapers reported that nearly all two-story buildings were destroyed after the second earthquake that had happened in December (Ulus Newspaper, printed on 27th of December). Lahn (1946) mapped the earthquake fault, and also prepared the earthquake risk map reporting also three different active faults. The first passed through Edremit County in the south and Zivistan (Elmalı), the second active fault was located between Van center and Kurubaş village, and finally there was an active fault line between the İskele district and Sıhke Lake to the north.

The Beyüzümü fault forms the contact between Paleocene-Eocene limestones and Quaternary units in this area (Fig. 2). Continuing eastward, the area lying between north of Beyüzümü village and the landfill site of the Van City, is the location where the morphology and structural features are best observed. The unit, which is located around the Beyüzümü village and named the "Beyüzümü terrace", is offset by normal faults in many areas (Fig. 5c–d). It forms a contact relationship between the Miocene Van Formation and the Quaternary Lake Van terraces in this area, and tilts the terrace deposits varying between 20° and 70° (Fig. 5 e-f). The Beyüzümü fault dips northward and forms mega scale drag folds on terrace deposits at the basement. The deformation, which is created by the fault on Quaternary terrace deposits and the morphological data, indicate that the Beyüzümü Fault has been active during the Holocene.

2.4.2. The Van Fault Zone

The Van Fault Zone (The Everek Fault) has caused many destructive and big earthquakes in the Van region (e.g. Van-Tabanlı Earthquake, Mw: 7.2, October 23rd, 2011 (KOERI, 2011). Based on national and international seismological observations, the Tabanlı (Van) earthquake nucleated at a depth of 16 km, 30 km north of Van City, and caused a 15 cm vertical displacement (Akyüz et al., 2011; Emre et al., 2011; Koçyiğit, 2013; Mackenzie et al., 2016). Both the historical and instrumental records have shown that two earthquakes with magnitudes equal or greater than 7 had occurred in Turkey within last 100 years on this thrust fault.

The Van Fault Zone is a 70 km long, northwest dipping, and approximately N70°W striking thrust fault (Fig. 4) (Akyüz et al., 2011; Emre et al., 2011; Koçyiğit, 2013, Mackenzie et al., 2016). Recent underwater studies outlined by Özalp et al. (2016) propose that the main coseismic fault (Van Fault) extends through the Lake Van for about another 9 km. It is formed by two different segments at the west and east. The western segment starts from Bardakçı village in the west and with a strike varying between E-W and N70°W until Aşıt village in the east (Fig. 4). The western segment forms a tectonic contact between the two units by thrusting the Van formation (Miocene) on to the lake terraces (Pleistocene) in some areas. InSAR observations reveal that an additional rupture occurred along a tear fault to the west of Lake Erçek that pinpoints the eastern end of the rupture (Akoğlu et al., 2018). Western segment of the Van Fault is cut by the splay fault (Kozluca fault) near the western part of the Lake Erçek (Akoğlu et al., 2018). The Beyüzümü (Bostaniçi) fault joins with the main Van fault to the north at depth (Doğan and Karakaş, 2013; Mackenzie et al., 2016; Akoğlu et al., 2018) however this fault and its relationship with our proposed Kozluca fault in the east is also unknown (Akoğlu et al., 2018) (Fig. 4).

The eastern segment extends until the Gedelova village and 25 km to the south of the Erçek Lake in the east. Generally, the fault can be morphologically traced within the Alaköy Formation (Fig. 6a–b). It forms a tectonic contact between the two units (the Alaköy formation

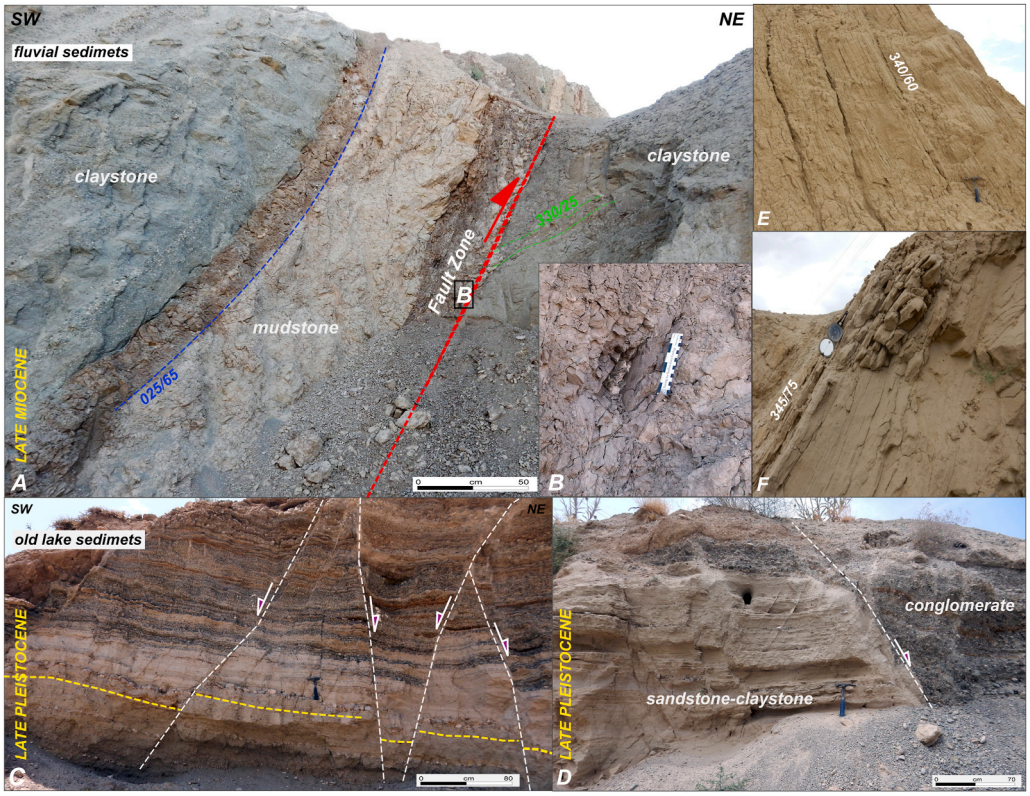

Fig. 5. a) The view of the Beyüzümü fault within old terrigenous deposits, b) close up view of fault plane c-d) normal fault that developed within the Beyüzümü terrace, e-f) the inclination that occurs on sandstone and much Dreissensia sp. levels.

and lake deposits) (Fig. 2) as it was observed in the western segment. It cuts Pliocene aged conglomerate-sandstone deposits and forms offsets varying in 20–50 cm (Fig. 6c–d). Similarly, the Van fault zone controls the northern margin of the Everek Basin where the Van City is located. Van Fault Zone or the Everek Fault are claimed to be reverse (Koçyiğit, 2013) or a blind thrust fault (Özkaymak et al., 2011).

2.4.3. The Yeniköşk Fault

The Yeniköşk Fault is an approximately 13 km long, south dipping thrust fault (Fig. 4). It starts near Yeşilköy village located on north of Van City and extends to Kasımoğlu village to the east. It was first defined in the Active Fault Map of Turkey (Emre et al., 2013a) (Fig. 4). Its direction varies between E-W and N80°W, forming a tectonic contact between the basement rocks and the Pliocene-Pleistocene deposits in the east, along its strike (Fig. 2). The morphological signature of the fault can be traced to the west.

The Yeniköşk Fault controls the southern margin of the Karasu Basin located north of the Van City. Sudden slope failures formed on this hill suggest that the fault is morphologically active. The late Miocene fluvial sediments in this area were deformed, faulted and folded along the eastern part of this fault (Fig. 7a). These deposits dip to the north at an angle of 78°, and secondary faults developed in the hanging wall. This fault does not cut the basalts that cover the Miocene sediments (Fig. 7a). The fault extends in an E-W direction on the east part, while in a N40-50°E trend in the west. In the western part of the region, some normal faults are observed in the Pliocene-Pleistocene terrace deposits

Fig. 6. a) The reverse dip-slip Van Fault zone which cuts old terrestrial deposits, b) close up view of fault plane, c-d) Van Fault Zone which cut late Miocene aged terrestrial deposits.

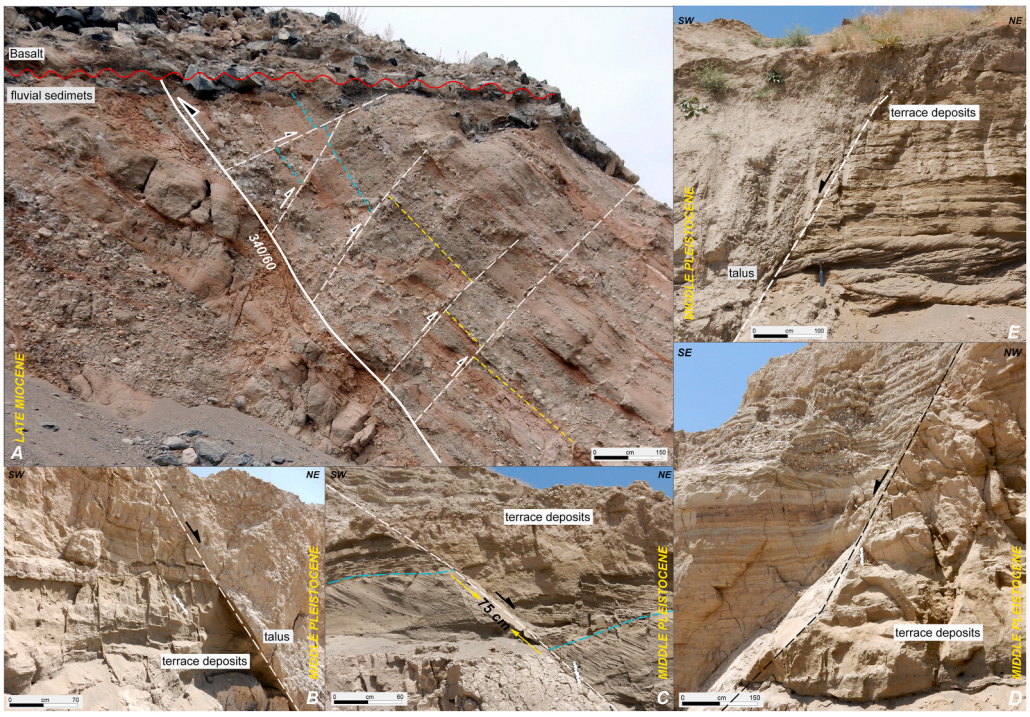

Fig. 7. a) Sudden reverse dip-slip and second order faults which cut Kurtdeliği formation clastics, b) first and second order normal faults cutting the Alaköy formation, c-d) normal faults which cut Pleistocene units in the upper layers.

(Fig. 7b–c). These faults have caused 75–100 cm displacements in the sediment layers (Fig. 7b–d). Additionaly, fault-front deposits characteristic for normal faults have been observed in this area (Fig. 7c–e). Thanks to the foundation excavations in the region, we observed that the fault cuts and deforms the river deposits and terrace levels of the Lake Van (Fig. 8a–b). There are 15–20 cm offsets in these deposits and the main fault strikes N40°E (Fig. 8a–b).

2.4.4. The Çolpan Fault

The Çolpan Fault, first named by Koçyiğit (2013), constitutes the southeastern boundary of the northeastern extension of the Van Lake (Fig. 4). It is an approximately 20 km long, left lateral strike slip fault, with a NE-SW thrust component (Fig. 4). Starting from Çolpan village, it can be morphologically traced until the eastern end of Ermişler village. Its morphological signature is uplifted terrace deposits where slope failures are common and the strata of these deposits exhibit drag folds (Fig. 9a–b). It also forms the tectonic contact between the stratigraphical units of the basin.

Along the fault extension, there are Pleistocene fluvial-lacustrine deposits characterizing the high-energy environment deposited in the southwestern part of the fault. The unit is cut by a N80°W trending reverse fault and offset vertically for ~2 m. The drag folds on the hanging wall are clearly observed (Fig. 9c–d). Conjugate normal dip-slip faults deform the ridge of the drag fold (Fig. 9a–e) forming a small graben structure. The deposits are folded approaching to the thrust plane. The slope angles of layers gradually increase towards the fault

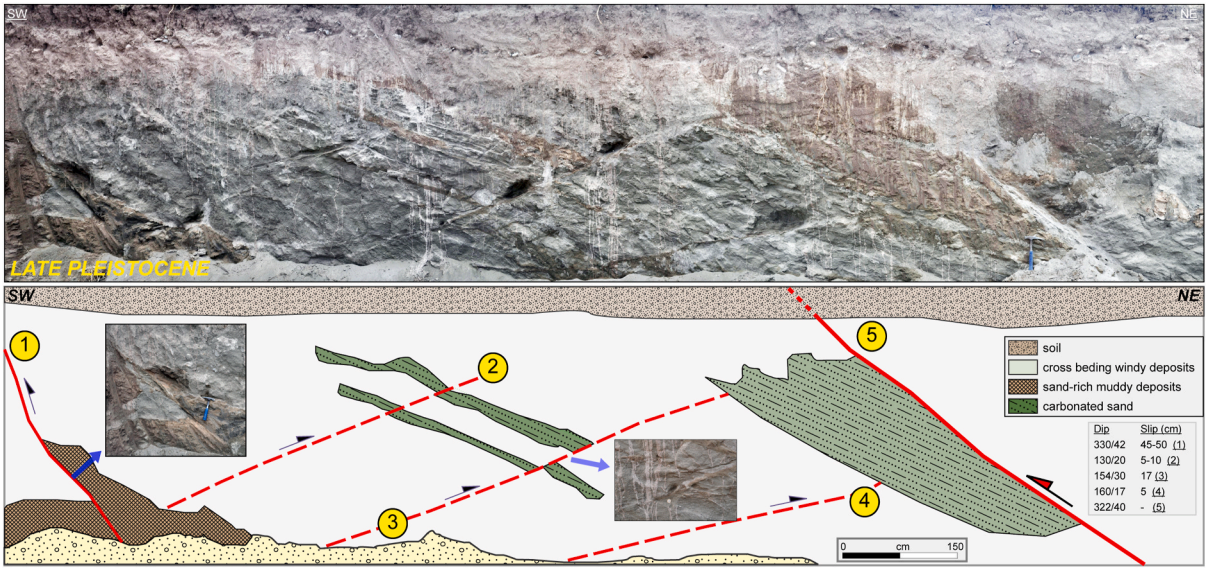

Fig. 8. a) The first and second order faults that cut Quaternary deposits, b) sketch up of the photography.

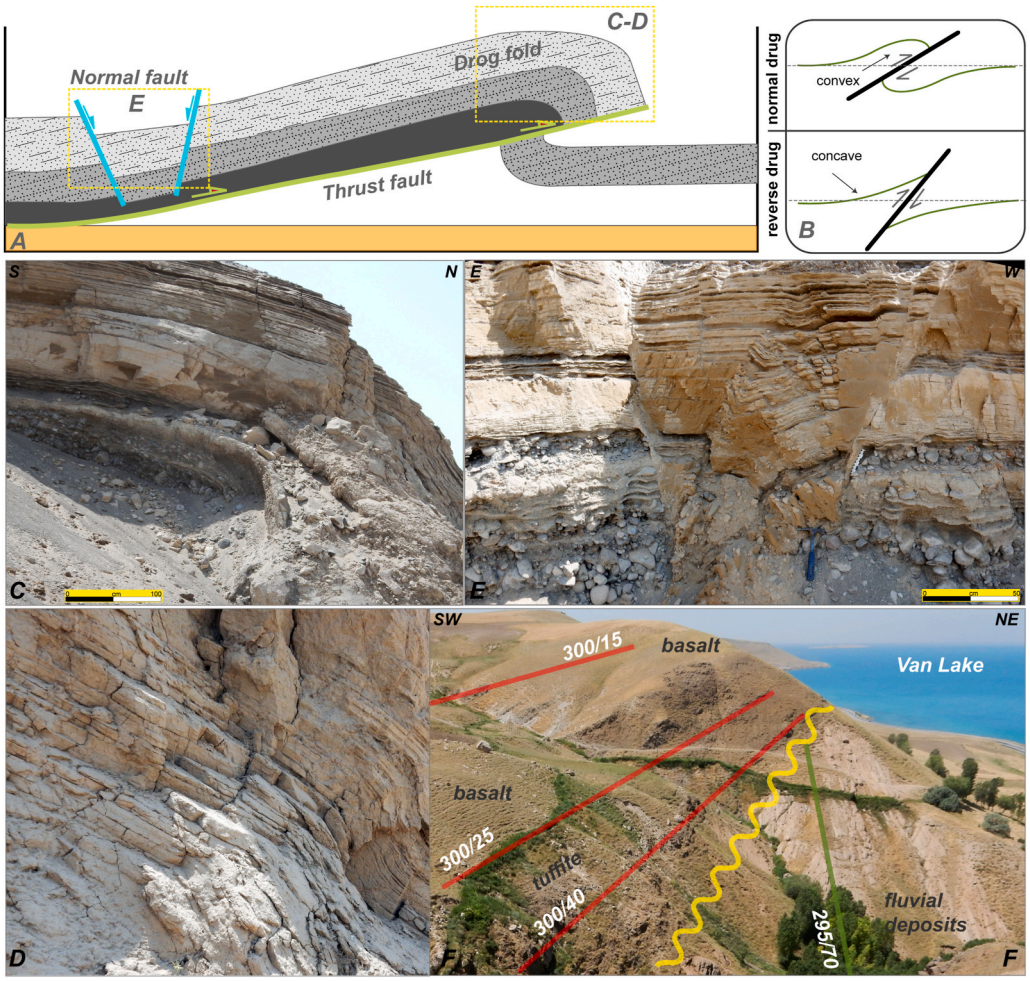

Fig. 9. a-b) Reverse dip-slip faults cutting the lake and river deposits and the offsets within lake deposits, and schematic section of the location, c-d) drag folds and offset lake deposits, e) normal fault cutting lake deposits, (f) relationship of lithology in the vicinity of Ermişler village.

plane. The strike of the main fault is E-W, and the strikes of the second order faults vary between N30°-60°E.

The long term deformation of the region is observed in the Ermişler Village. Here the clastic unit of the Kurdeliği formation is unconformably overlain by thick basalt flows of late Miocene (7.1 ± 0.2 Ma K/Ar). The overall strata trending roughly WNW-ESE are progressively tilted to the south, starting 15° at the uppermost basalt flow to 30° to basal tuffites and reaching 70° at clastics (Fig. 9f). This observation indicates that the Çolpan fault is a prominent tectonic structure continuously deforming the region at least since late Miocene.

2.4.5. *The Erciş Fault*

Running about 50 km between Ulupamir village (Erciş) and Yumaklı village (Muradiye) to the northeast, the Erciş Fault is one of the main faults in the Lake Van Basin. It is a right lateral strike slip fault with normal component and a strike of N30°-50°W (Fig. 10a–d). The Erciş fault is highly segmented and cuts the Girekol volcano in the west, and its trace within basalt flows are distinctive (Şaroğlu, 1986). Erciş fault cuts and offsets fluvial and lacustrine terraces along its trace where syn and post-depositional deformation is observed within the sections of these late Pleistocene deposits (Fig. 10a–f). The vertical offset on the secondary faults are measured up-to 150 cm (Fig. 10a–f). The fault planes preserving the slip indicators can be observed (Fig. 10c). There are also morphologically observed pressure ridges and river offsets along the fault in the same area. In addition to its sedimentological and paleontological background (Üner et al., 2017), the lacustrine terrace deposits along the Erciş Fault host important clues about seismic activity during the late Quaternary, namely seismites. These deformational structures that are formed during earthquakes in unconsolidated sediments are very rare geologic phenomena (Üner et al., 2017, 2019). It is possible to see these deformational structures caused by the seismic activity on the Erciş Fault along the Zilan River (Fig. 10g). These structures are formed by earthquakes of magnitude ≥5 under suitable conditions. Towards the southeast (in the Ünseli county), the fault cuts and offsets the southern margin of the Etrusk Volcano and forming ~11 km right lateral cumulative offset (Copley and Jackson, 2006).

Historical and instrumental records of earthquakes indicate the presence of more than one destructive earthquake in the Erciş region. Historical records indicate that there was an earthquake on October the 3rd 1276 that affected Erciş and Ahlat and their surroundings, and caused serious destruction (Ambraseys, 2009). According to instrumental records, two earthquakes with $M_w > 5$ occurred in Erciş in 1941 and 1971. It was reported that 192 people had lost their lives and a total of 36 villages were ruined in 1941 Earthquake (Eyidoğan et al., 1991; Pınar and Lahn, 1952). The Erciş Fault is one of the main faults of the region that have a high possibility to generate a near-future earthquake, with an estimated earthquake recurrence interval of 125–250 years (M ≥ 5) (Üner et al., 2019).

3. Kinematic analysis

Kinematic (paleostress) analysis refers to numerous methods used to determine the regional strain tensor consistent with geological structures by combining the direction of fault populations according to fault-

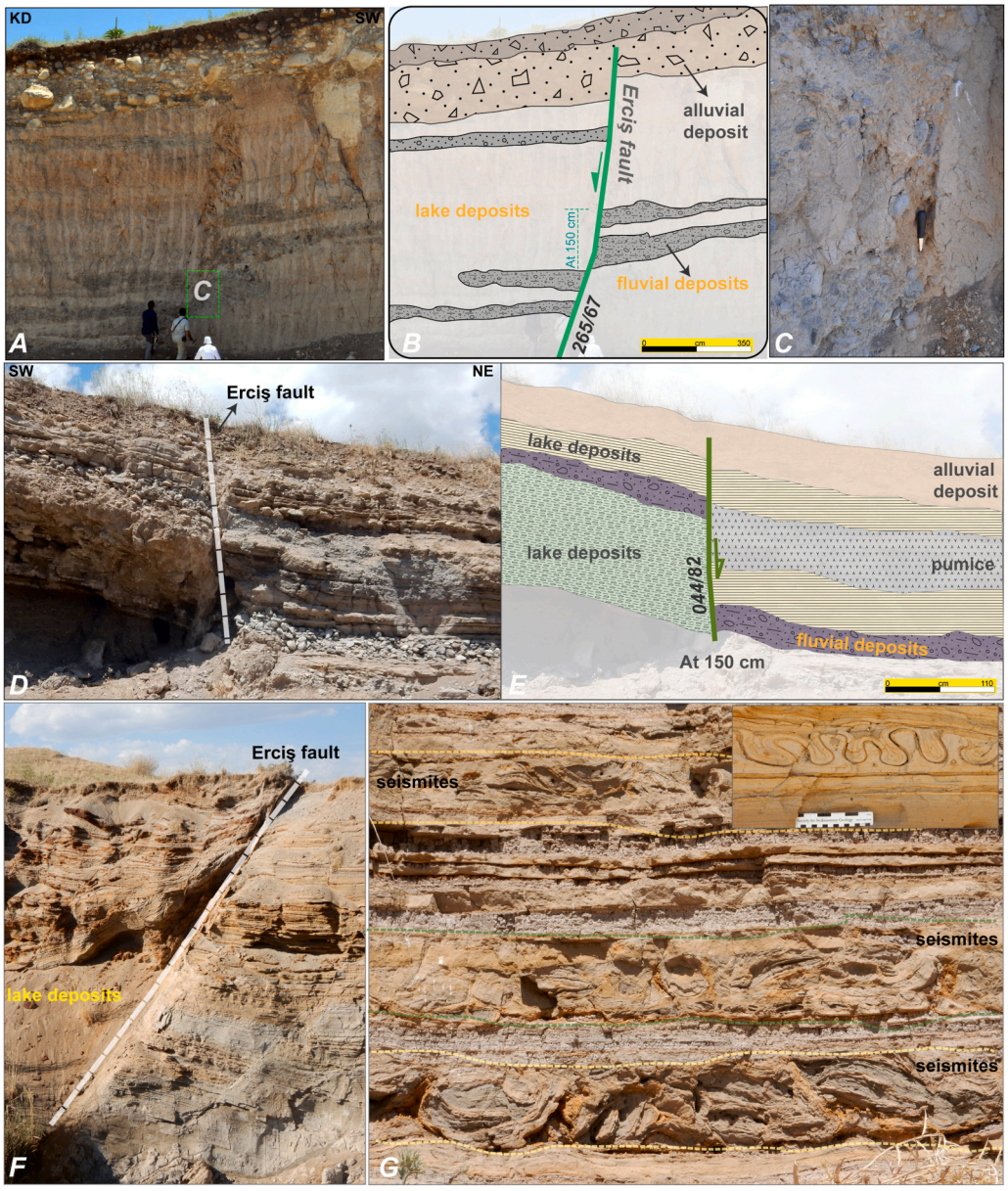

Fig. 10. a) The Erçiş fault cutting fluvial and lake sediments, b) sketch up photography A, c) view of fault plane, d-f) right lateral strike slip fault with normal component in N46W direction (Erciş Fault), d) sketch up photograpy C, g) earthquake structures formed within the lake sediments (seismisite).

slip data (i.e. Angelier, 1984). Various techniques have been proposed to estimate the strain tensors (Angelier, 1984; Michael, 1984; Reches, 1987; Fry, 1999; Delvaux and Sperner, 2003). Most of these methods sample the fault that slipped independently within the homogeneous stress area and try to represent the direction of the maximum shear stress on the fault plane by recorded fault-slip data. Detailed mapping of the Lake Van Basin offer a good basis for the investigation of such structural relationships. In this study, the stress field orientations of the mapped faults are estimated in order to determine the kinematic framework of faulting that operated during the Neogene–Quaternary evolution of the LVB.

We analyzed the fault kinematic data measured at different locations around the LVB using the Angelier stress inversion method (Angelier, 1984, 1990, 1994) (Fig. 11). All data were computed using the MyFault software. For each fault with slickenside striations, (a) fault plane direction (b) dip direction, (c) dip amount, (d) rake, (e) striation trend, and (f) rate referring to the quality of the measured data were computed. These are the directions of the three principal stresses ($\sigma1 > \sigma2 > \sigma3$) and the relative magnitudes for the principal stress axes, expressed by the axial ratio $\varphi = (\sigma2 - \sigma1)/(\sigma3 - \sigma1)$, with $0 < \varphi < 1$ (Angelier, 1994). The stress regime is determined by the nature of the vertical stresses as follows; extensional when $\sigma1$ is vertical, strike-slip when $\sigma2$ is vertical and compressional when $\sigma3$ is vertical. Delvaux et al. (1997) suggest that the stress regimes also vary by the function of the stress ratio, which ranges from 0 to 1: radial extension ($\sigma1$ vertical, $0 < \varphi < 0.25$), pure extension ($\sigma1$ vertical, $0.25 < \varphi < 0.75$), transtension ($\sigma1$ vertical,$0.75 < \varphi < 1$ or $\sigma2$ vertical, $1 > \varphi > 0.75$), pure strike-slip ($\sigma2$vertical, $0.75 > \varphi > 0.25$), transpression ($\sigma2$ vertical, $0.25 > \varphi > 0$ or $\sigma3$vertical, $0 < \varphi < 0.25$), pure compression ($\sigma3$ vertical, $0.25 < \varphi < 0.75$) and radial compression ($\sigma3$ vertical, $0.75 < \varphi < 1$).

The stress calculated by the inversion of heterogeneous data does not characterize the real state of stress. Field observations are important for determining paleostresses from heterogeneous fault-slip data and to distinguish the different paleostress phases. Heterogeneous sets of fault-slip data were separated into subsets in the field as much as possible. Additionally, the allowable maximum misfit angle (ANG) and the

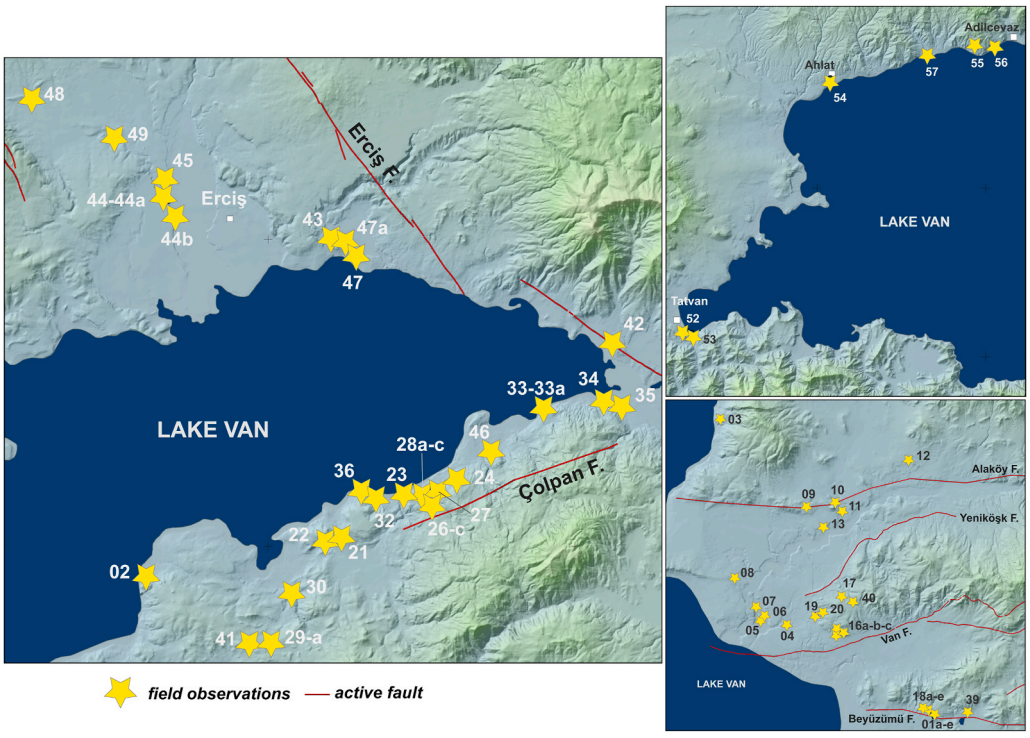

Fig. 11. The field observation locations in the Lake Van Basin.

maximum quality estimator (RUP) values (Angelier, 1994) were also taken into account. In the analysis, the ANG (i.e. maximum misfit angle between the observed slip and computed shear stress direction) was taken as 15° and the RUP was taken as 45°. The faults, which exceeded these values, were excluded and recomputed as separate tensors.

4. Results

The fingerprint of the tectonic evolution of the LVB is preserved in the faulted rocks within the basin stratigraphy. The kinematic datasets consist of striated minor and major fault planes that can be classified temporally according to the age of the host rock. These datasets were then analyzed by means of graphical and mathematical methods, revealing the temporal variation of the primary axis of the stress components deforming the region during late Miocene-Quaternary interval. The change in principal stresses is well determined by using the data obtained from geological units that have different ages and litologies, allowing for temporal discrimination.

At 27 different locations around the LVB, a total of 245 observations on fault planes were obtained to perform the kinematic analysis (Fig. 11). These data were collected from natural and artificial outcrops all around the basin. We devided the kinematic data temporally into: (I) Phase 1 (late Miocene), (II) Phase 2 (Middle Pleistocene) and (III) Phase 3 (late Pleistocene). By temporal classification, we deduced the time and space variation of the stress regime that dominates the tectonic development of the Basin.

4.1. Phase 1 (late Miocene)

Phase 1 which represents the state of effective regional stress during the late Miocene is well evidenced in various localities at Van, Çolpan, and Everek. The kinematic data in these areas have been collected within the Kurtdeliği formation along the Van Fault Zone (VFZ), the Yeniköşk fault (YF), the Beyüzümü fault (BF), and the Çolpan fault (CF) (Fig. 1) which are located in the eastern part of the Lake Van Basin. Phase 1 is characterized by NE–SW and NW–SE, oblique strike-slip faults, and NE-striking reverse faults that cut and deform the Miocene volcanic and sedimentary rocks (Table 2, Fig. 12).

The inversion of fault-slip measurements (VFZ, YF, CF) for early Phase 1 defines steeply plunging $\sigma_1$axes (66° and 51°), but gently plunging σ_3 axes (04°and 15°) (Location 16-19-29a) (Table 2, Fig. 12). This suggests strike slip faulting with contraction in N80°W direction and extensionin N10°E direction. The results from the fault slip measurement along these faults (VFZ, YF, BF, CF) for the later period of Phase1 define steeply plunging σ_1 axes (47°), but gently plunging σ_2 and σ_3 axes (22° and 40°) (Location 20-32-41-41c) (Table 2, Fig. 12). The results suggest an approximately N40°W trending contraction associated with at least N50°E trending extension.

The kinematic data obtained from Miocene sediments are classified according to stratigraphic relations were evaluated by considering these relations. The results indicated that NW or NE trending oblique and thrust faulting were consistent with a transtension zone ($\varphi = 0.75–0.88$), except for the CF, BF and VFZ. On the other hand, the direction of compression and extension are different between the early and late Miocene.

4.2. Phase 2 (Middle Pleistocene)

Phase 2 is characterized by strike-slip and thrust faults that deformed the fluvial and lake deposits (384 ± 9.1 ka). The analyzed dataset is collected from faulted sections in 12 different locations. The fault zones in CF, AF, BF and EF show right and left-lateral strike-slip movement which seem to form conjugate sets, since they operated at the same time.

The observations from east of the Lake Van Basin along the faults indicate that the minimum stress axis (σ_3) is steeply plunging (Table 2). The orientation of σ_2 axes is 261°/01°. This suggests a contraction along N10°W direction. Along the strike of the EF, the fault-slip analysis defines an approximately vertical $\sigma_2$with a plung of 85°. The σ_1 and σ_3 are almost horizontal, and plung at 01° and 05°, respectively. The results suggest an approximately N40°W directed contraction associated with N50°E extension (Table 2, Fig. 13).

The kinematic analysis results along the CF indicate that a

Table 2
Results of palaeostress analysis from measurements of slickensides in the study area (see Fig. 11 for locations).

Phase	Name of fault	Location no	Type of fault	Number of slip data	σ_1	σ_2	σ_3	φ	ANG
D1	CF	29	Reverse	21	298/66	129/24	037/04	0.76	0.4
	VFZ	16	Normal-slip	8	166/51	264/07	359/39	0.88	0.5
	YF	19	Reverse	8	331/31	230/18	114/54	0.58	0.2
	YF	20	Reverse	12	046/02	137/19	310/71	0.67	0.4
	CF	32	Strike-slip	10	171/68	330/20	062/07	0.60	0.3
	CF	41	Strike-slip	6	287/47	162/29	054/29	0.73	0.2
	BF	41c	Reverse	10	206/28	335/49	100/27	0.84	0.5
D2	EF	47	Reverse	10	259/61	157/7	63/28	0.72	0.1
	YF	10	Reverse	8	020/7	288/11	142/77	0.38	0.2
	CF	33	Reverse	8	106/34	001/22	244/48	0.96	0.2
	EF	44	Reverse-Slip	6	173/71	310/14	043/12	0.84	0.2
	Tatvan	52	Strike-slip	6	012/24	276/14	159/62	0.15	0.3
	CF	26a	Reverse	8	196/03	287/05	196/03	0.6	0.2
	EF	42	Strike-slip	10	197/49	330/30	075/24	0.63	0.2
	BF	39	Reverse	10	206/28	335/49	100/27	0.86	0.1
D3	BF	01	Reverse	15	346/77	132/11	224/07	0.65	0.3
	YF	06	Reverse	9	132/85	026/01	296/05	0.47	0.3
	AF	09	Reverse-Strike-slip	8	225/03	357/85	135/04	0.44	0.3
	YF	07	Reverse-Strike-slip	7	053/39	280/40	166/26	0.20	0.4
	YF	24	Reverse-Strike-slip	13	149/87	299/03	029/02	0.04	0.4
	CF	26	Reverse	8	096/70	342/08	250/18	0.71	0.2
	CF	28b	Reverse	7	198/22	080/49	303/33	0.48	0.4
	CF	34	Reverse	6	354/01	257/85	087/05	0.52	0.4
	CF	36	Reverse	6	351/03	261/01	152/87	0.76	0.2
	CF	38	Reverse	9	354/13	165/77	263/02	0.52	0.2
	EF	47a	Normal-slip	7	266/01	358/55	175/35	0.37	0.4
	Tatvan	53	Strike-slip	9	012/24	276/14	159/62	0.15	0.3

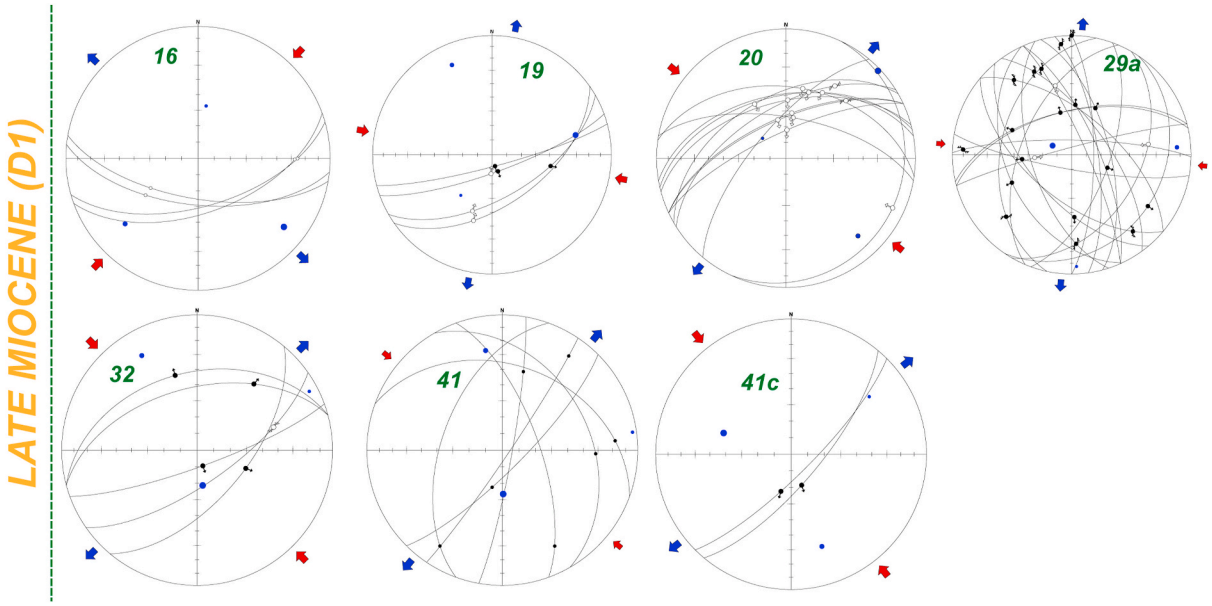

Fig. 12. Paleostress analyses carried out on the late Miocene units.

transpression regime was operating east of the Lake Van Basin (φ = 0.76) in the early Pleistocene (Table 2). On the other hand, the data from north of the Lake Van Basin along the EF suggest that NW or NE trending strike-slip faulting is consistent with a NE–SW transtensional regime (φ = 0.89) in the middle Pleistocene (Fig. 13).

4.3. Phase 3 (late Pleistocene)

The old terrace levels of Lake Van are widely exposed in the eastern and northern parts of the Basin. These sediments have undergone extensive deformation and were uplifted by faults located in the Basin. However, while the eastern part of the Basin is controlled by thrust faults (BF, VFZ, YF and CF), the northern and western part of this basin is dominated by strike-slip faults (EF).

The observations from the EF indicate that the intermediate (σ_2) stress axis is steeply plunging (Table 2), suggesting an approximately N15°W directed contraction associated with N75°E extension during Quaternary (Fig. 14). The fault-slip measurements for the YF and BF for the Quaternary period define steeply plunging σ_3 axis (62°) and gently plunging σ_1 axis (23°). The strike slip faulting with reverse component developed at around N10°W trending contraction with N80°E trending extension (Fig. 14). Along the strike of the YF, our results define an approximately vertical σ_3 plunging at 80°. The result suggests NNW–SSE contraction and WSW-ENE extension (Fig. 14).

This phase, which is evidenced by the youngest structures of the region, indicates transpressional deformation east of the Lake Van Basin

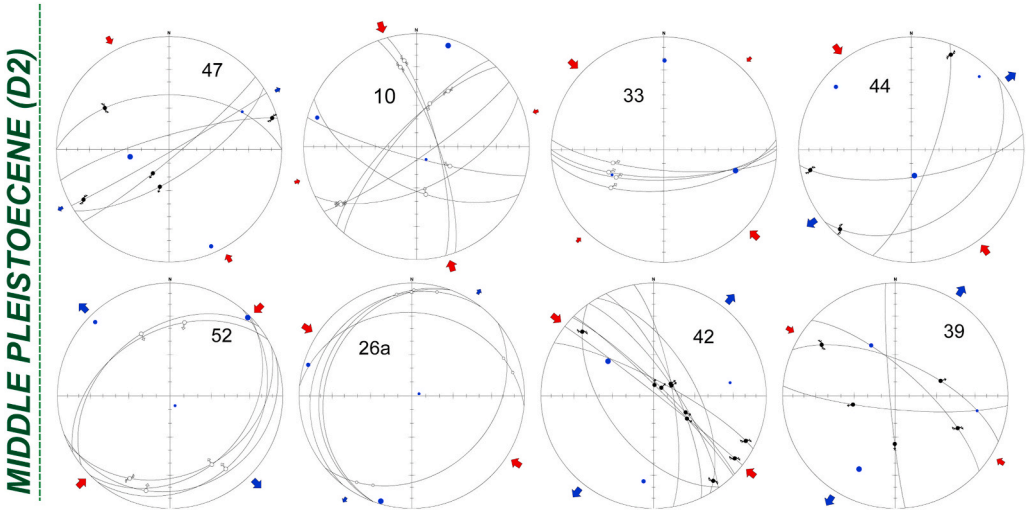

Fig. 13. Paleostress analyses of the faults carried out on the Middle Pleistocene strata.

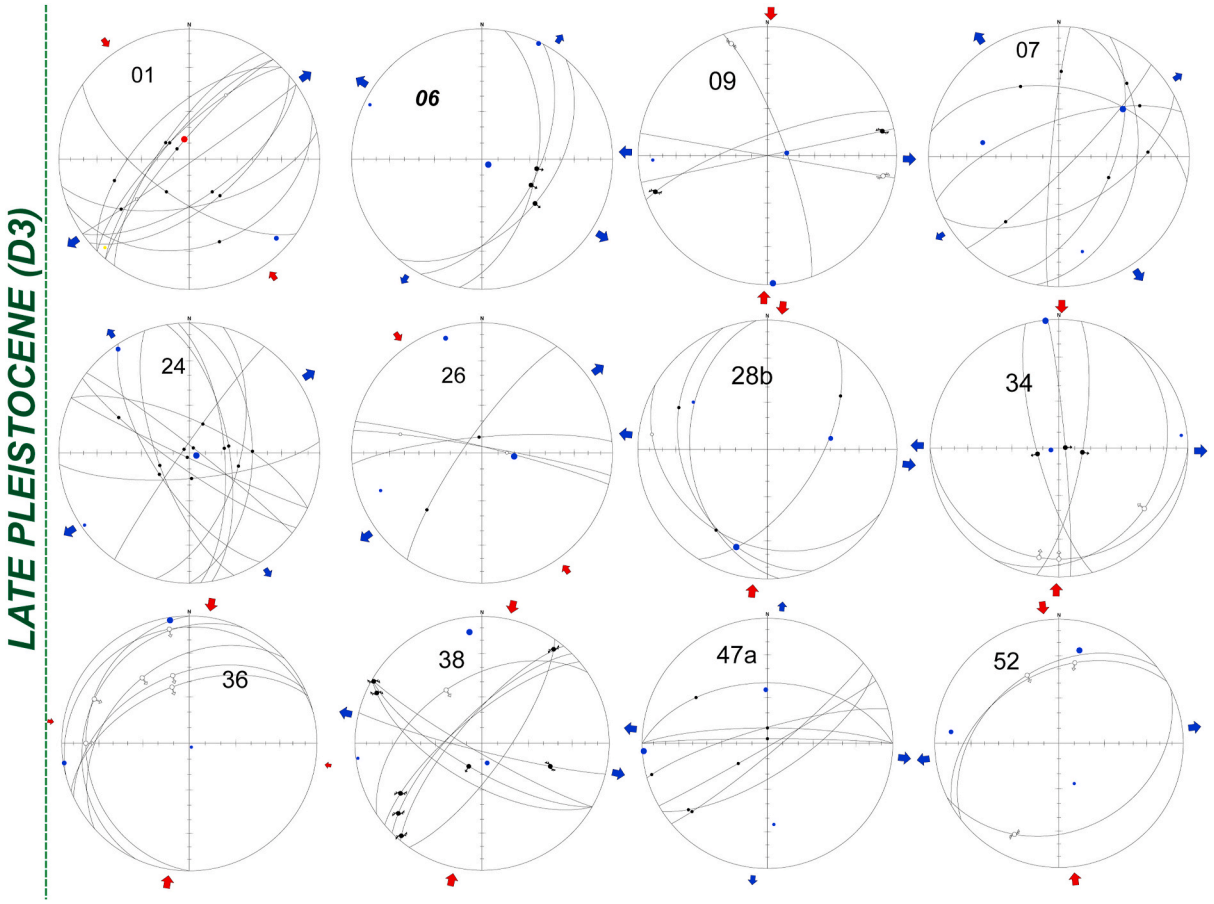

Fig. 14. Paleostress analyses of the faults carried out on the late Pleistocene strata.

($\varphi = 0.26$). Otherwise, the observations collected along the EF indicated that NW or NE trending strike-slip faulting was consistent with a NE–SW transtensional regime ($\varphi = 0.78$–0.87) in the late Pleistocene (Fig. 14).

5. Discussion and conclusion

The LVB is thought to have formed in the late Miocene-early Pliocene within the framework of the Arabia-Eurasia collision (Sengor and Kidd, 1979; Şengör et al., 1985; Dewey et al., 1986; Kocyigit et al., 2001). One of the deposits of this collision was the early Miocene-late Pliocene sedimentation (Aksoy, 1988; Acarlar et al., 1991). The Pliocene sediments are classified according to stratigraphic relations within the basin. These deposits are unconformably overlain by the Quaternary, old lacustrine (terrace) deposits. They are mostly confined to valleys and coastal areas with sections 3-25 meters displaying well-preserved sedimentary features and provide important clues for determining their depositional environments (nearshore lake, delta, beach and alluvial fan) (Üner, 2003; Görür et al., 2015). They expose at elevations ranging

from 1650 m to 1790 m (Fig. 15). Dating of these terraces was performed using the radiocarbon, OSL and $^{234}Th/^{238}U$ methods in previous studies (Kempe et al., 2002; Kuzucuoğlu et al., 2010, Görür et al., 2015). The $^{234}Th/^{238}U$ method was also applied in this study (Fig. 15). Here we report the oldest age determination so far for the lake terraces as 347 ka in the northeastern part of the Basin (Fig. 15). The deposit reaches 1700 m, about 43 m above the present lake level (Fig. 15). Relatively younger ages were obtained from two different localities of terrace deposits in east Lake Van Basin (203 ka-213 ka) which also comprimises the highest terraces that reach 1790 m in Beyüzümü and 1769 m in Yeşilköy (+110 m and +139 m relative elevation) (Fig. 15). Although the terraces are believed to represent periods of relatively higher water level of Paleo-Lake Van relative to its present lake level (Görür et al., 2015), the age and relative height of the lake terraces indicate differential uplift is in effect for the region which remains to be solved.

Mapping of active faults located in the Lake Van Basin (Emre et al., 2013a) and information on their structural characteristics have been reported in different studies (Koçyiğit, 2013; Dicle and Üner, 2017 Akkaya et al., 2015). In addition, active faults located within Lake Van were mapped by detailed seismic reflection studies (PaleoVan Project, Litt et al., 2009; Çukur et al., 2014, 2017; Özalp et al., 2016, Toker et al., 2017). While young sediments on the eastern and southern parts of the Basin are deformed by inverse faults, strike slip deformation occurs in the northern and eastern parts of the Lake basin. In the eastern part of the Basin, from south to north, the Gürpınar, Beyüzümü, Van, Yeniköşk, Alaköy and the Çolpan faults are located. These faults are reverse in character and control the eastern part of the young tectonics of the Basin. The 23rd October 2011 Earthquake (M_w: 7.2) occurred on a low angle reverse fault, which had not been previously mapped, and extends in a NE direction from offshore on to the land in the eastern part of the Lake (Özkaymak et al., 2011; Doğan and Karakaş, 2013; Akkaya et al., 2015). North of LVB, the Erciş and the Çaldıran faults restrict the basin from the north. Both faults are dextral strike slip in character. The Beyüzümü Fault, one of the significant faults located in the eastern part of the Lake Van Basin, is a 20 km long thrust fault (Mackenzie et al., 2016). It is one of the main reverse faults that control the deformation in this area. It was reported that the 1945 earthquakes took place on this fault (Lahn, 1946). Field studies carried out along the Beyüzümü Fault showed that the old lake terrace deposits located in this area were highly deformed. Terrace layers closer to the fault (230 ka) are tilted 75° southward. In addition, these deposits present 30 m elevation difference compared to layers with similar ages, indicating that the sampled unit were deformed and uplifted, as reported in previous studies (Mackenzie et al., 2016). The Çolpan Fault is located on the northeast margin of the LVB. Koçyiğit (2013) mapped the fault, but did not give any further information about structural characteristics. It is an approximately 20-km long reverse fault with a left lateral strike slip component. The long-term activity of the fault continuously deformed the late Miocene units of the basin tilting the strata up to 70° southward. Drag folds were obsered in various places on the hanging wall along the fault. Furthermore, the traces of faulting and deformation are observed within the lake terraces along the fault indicate that Çolpan Fault is still active.

Along the eastern and northern parts of the LVB, we undertook measurements along the fault planes. Kinematic analysis of the fault slips data reveals the tensional states that were effective during the late Miocene-Quaternary.

The Neogene–Quaternary evolution of the zone is characterized by variable wrench faulting to compression dominated transpressive systems, resulting in a complex fault pattern. We encountered three different deformation phases around the Lake Van Basin during the

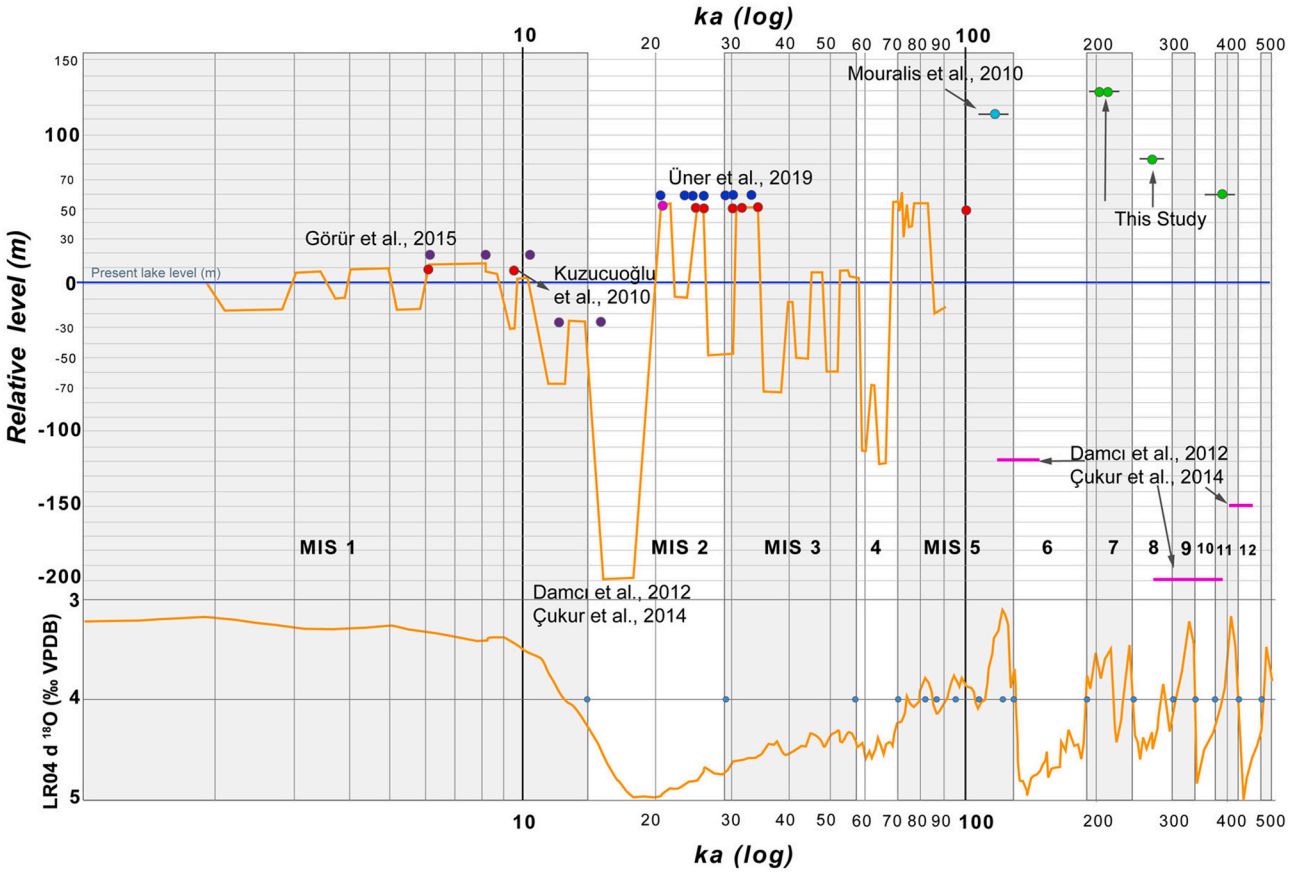

Fig. 15. Radiometric ages of the Lake Van terraces displayed in logarithmic time scale and suggestions for the lake level changes during the middle-late Pleistocene. The marine isotope curve and stages are from Lisiecki and Raymo (2005).

Neogene-Quaternary (Fig. 16).

As mentioned earlier, the Miocene river sediments expose in a large area in the east of the LVB. These sediments were affected by extensive deformation in the region and folded to the east/northeast of this Basin. The axes of these folds generally trend NE-SW.

According to the kinematic data obtained from late Miocene deposits (Phase 1), the largest principal stress (σ1) axis and the smallest principal stress (σ3) axis were calculated as 140 ± 15° and 240 ± 20°, respectively (Table 2). This implies a tectonic regime (strike slip fault) in which the largest principal stress axis (σ1) and the smallest principal stress axis (σ3) are nearly horizontal, and the intermediate stress axis (σ2) is in vertical position. The direction of compression is in N70-40°W (Fig. 16). However, the extensional direction is N20-50°E (Fig. 16). At the same time, it shows that dominant the tectonic feature in Miocene in the LVB is a right lateral strike slip fault (transtensional) with a normal component that developed under the NW-SE compressional direction (Fig. 16).

The second stage of deformation (Phase 2) is characterized by compressional deformation that is controlled by the vertical σ_3 stress with NW-SE contraction strain axes (Fig. 16). The traces of this deformation phase are clearly observed in the fluvial and lake deposits (384 ± 9.1 ka). During this stage, the northeast margin of the LVB was controlled by the CF and the EF that seems to form a conjugate set (Fig. 16). We performed the kinematic analysis at three locations along the CF, and determined the minimum stress (σ_3) as steeply plunging (Table 2). The result suggests a N10°-40°W contraction and there were extensions associated with this contraction in the northeast margin of the basin (Fig. 16). The EF bounds the northern margin of the LVB and extends parallel to the block boundary (TIP and LCW, Reilinger et al., 2006, Djamour et al., 2011) (Fig. 15). Along the strike of the EF, the results suggest an approximately vertical σ_2 stress plunging at 85°, and a N40°W directed contraction associated with at least N50°E extension (Fig. 16). According to our analysis, the compressionnal tectonic regime was dominated to the east of the LVB, while the northern part of the basin was dominated by a transtensional tectonic regime at this stage of deformation. The reason for this difference in deformation is that the Erçiş Fault is caused by the block boundary fault. Because, the northern LVB is controlled by the strike slip fault (Çaldıran and Erçiş faults) that participate with the belt-parallel component of the relative plate motion (Jackson, 1992).

The youngest stage of deformation (i.e., Phase 3) is determined for the late Pleistocene period. This phase is evidenced by the youngest structures of the region, and indicates a transpressional deformation in the eastern paert of the Lake Van Basin (φ = 0.48). Otherwise, our computed results along the EF would indicate that NW or NE trending strike-slip faulting is consistent with a NE–SW the transtensional stress regime (φ = 0.48) in late Pleistocene (Fig. 16).

LVB which is bordered by the Çaldıran Fault to the north and the Bitlis-Zagros Suture Zone to the south at located in the eastern Anatolian region. This regional deformation represents pure intracontinental deformation between the Arabian and the Eurasian plates. This region, elastic block models based on GPS data (e.g., Reilinger et al., 2006) suggest two broad tectonic blocks, the Caucasus and Iran blocks the Iranian block being disected by N–S faults (Khorrami et al., 2019). The boundary between the deforming Iranian block and the Arabian plate is defined as the Bitlis–Zagros Belt. Additionally, Recent models using data from the increasing number of GPS surveys by Khorrami et al. (2019) describe, NW Iran–Caucasus–eastern Turkey, the deformation is partitioned between almost pure shortening across the southern Greater Caucasus, presumably on the Main Caucasus thrust fault, and right-lateral strike-slip along the North Tabriz Fault, Gailatu–Siah Cheshmeh–Khoy and Çaldıran Fault system. This studies show that, based on observations from kinematic data from LVB, the transpression regime appears to have been dominated with compressional movement relatively in the east part of the basin. The reason for this compressional to appear more in the southern parts of the basin, it is the restriction of the Iran Block, which also includes the LVB, by the strike-slip Çaldıran and Erciş faults. The Erciş Fault extends parallel to the block boundary between TIP and LCW.

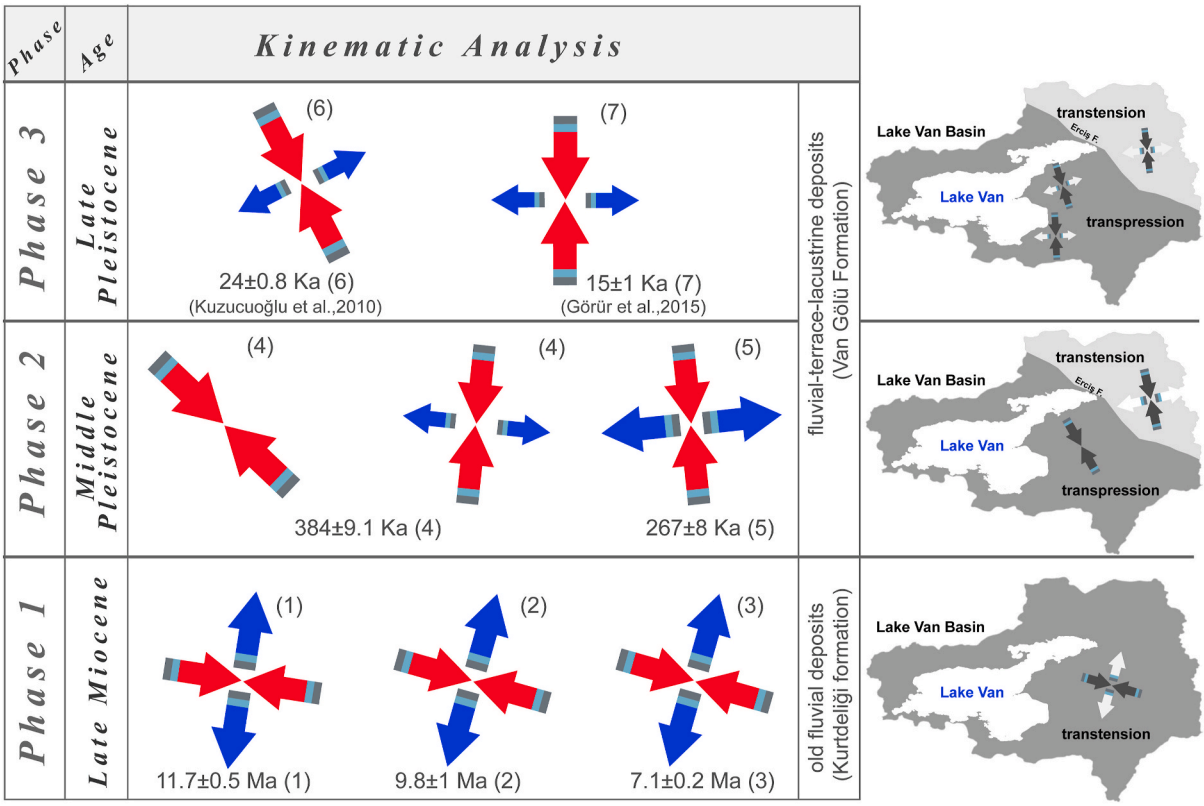

Fig. 16. The temporal evolution of principal stress direcitons obtained by the kinematic anaylsis of fault groups.

Şengör and Kidd (1979) have previously suggested that active shortening and crustal thickening gave rise to the numerous thrusts in the Lake Van region (Fig. 16). The structural development of the LVB occurred during the Plio-Quaternary period, and continues today (Sengor and Kidd, 1979; Şengör et al., 1985; Dewey et al., 1986; Kocyigit et al., 2001; Sengor et al., 2008; Çukur et al., 2013; 2014a, 2017). Different tectonic regime phases have been active during the Plio-Quaternary period (Çukur et al., 2017; Toker et al., 2017). Dhont and Chorowicz (2006), based on the observations from digital elevation model images from eastern Anatolia, claim that the orientations of the tectonic and volcanic structures fit with the tectonic regime characterized by N–S shortening and E-W elongation. Recent studies show that, based on observations from seismic reflection data from Van Lake, the extensional regime appears to have been replaced with compressional movements relatively recently in the central part of the Basin (Çukur et al., 2017). Transpression and transtension are strike-slip deformations that deviate from simple shear because of a component of, respectively, shortening or extension orthogonal to the deformation zone (Dewey et al., 1998). The tectonic regime of the Van Basin was transtensional in the late Miocene. It seems that the transpression regime dominates the early Pleistocene, in which we observed a locally transtensional regime. The late Pleistocene tectonic transpressional deformation that develops under compression in NNW-SSE and extension in ENE-WSW directions (Fig. 16) might be related to the change in the regional-scale plate geodynamics (Çukur et al., 2017).

CRediT authorship contribution statement

Azad Sağlam Selçuk: Conceptualization, Methodology, Investigation, Formal analysis, Writing - original draft, Project administration, Funding acquisition. **Mehmet Korhan Erturaç:** Methodology, Formal analysis, Investigation, Resources, Writing - review & editing. **Gürsel Sunal:** Data curation, Writing - review & editing. **Ziyadin Çakır:** Data curation, Writing - review & editing.

Declaration of competing interest

The authors declare that they have no known competing financialinterestsor personal relationships that could have appeared to influence the work reported in this paper.

Acknowledgements

The authors are particularly grateful to Rob Reilinger for critical comments and English editing. We also gratefully thank Editor and anonymous reviewers for providing critical comments that significantly improved the manuscript and also special thanks to Levent Selçuk who contributed to the fieldwork. This study was financially supported by the TUBITAK Scientific Research Project (114Y274).

References

Acarlar, M., Bilgin, A., Elibol, E., Erkal, T., Gedik, İ., Güner, E., Hakyemez, Y., Şen, A., Oğuz, M., Umut, M., 1991. Geology of Van Lake East and North, MTA Report No: 9469. Ankara, 94s (unpublished).

Akkaya, İ., Özvan, A., 2019. Site characterization in the Van settlement (Eastern Turkey) using surface waves and HVSR microtremor methods. Journal of Applied Geophsics 160, 157–170.

Akkaya, İ., Özvan, A., Tapan, M., Şengül, M., 2015. Determining the site effects of 23 October 2011 earthquake (Van province, Turkey) on the rural areas using HVSR microtremor method. Journal of Earth System Science 124 (7), 1429–1443.

Aksoy, E., 1988. Stratigraphy and Tectonics of the East-Northeast Region of Van Province. Doctorate Thesis. Fırat University, Institute of Science, Elazığ, Turkey, p. 171 (unpublished).

Akoğlu, A.M., Jónsson, S., Wang, T., Çakır, Z., Doğan, U., Ergintav, S., Osmanoğlu, B., Feng, G., Zabcı, C., Özdemir, A., Emre, Ö., 2018. Evidence for Tear Faulting from New Constraints of the 23 October 2011 Mw 7.1 Van, Turkey, Earthquake Based on InSAR, GPS, Coastal Uplift, and Field Observations. Bulletin of the Seismological Society of America.

Akyüz, S., Zabcı, C., Sancar, T., 2011. 23 Ekim 2011 Preliminary Reports on Van Earthquake. Istanbul Technical University, Istanbul, Turkey.

Al-Lazki, A.I., Seber, D., Sandvol, E., Türkelli, N., Mohamad, R., Barazangi, M., 2003. Tomographic Pn velocity and anisotropy structure beneath the Anatolian plateau (eastern Turkey) and the surrounding regions. Geophys. Res. Lett. 30, 6-1/6-4.

Altıner, Y., Söhne, W., Güney, C., Perlt, J., Wang, R., Muzli, M., 2013. A geodetic study of the 23 October 2011 Van, Turkey earthquake. Tectonophysics 588, 118–134.

Ambraseys, N., 2009. Earthquakes in the Mediterranean and Middle East. Cambridge University of Press, New York.

Ambraseys, N.N., 2001. Reassessment of earthquakes 1900-1999 in the eastern mediterranean and the Middle East. Geophys. J. Int. 145 (2), 471–487.

Ambraseys, N.N., Jackson, J.A., 1998. Faulting associated with historical and recent earthquakes in the Eastern Mediterranean region. Geophys. J. Int. 133 (2), 390–406.

Ambraseys, N.N., Finkel, C., 1995. The Seismicity of Turkey and Adjacent Areas: A Historical Review, 1500-1800. M.S. . İstanbul: Eren Yayıncılık.

Ambraseys, N.N., Finkel, C.F., 2006. Turkey and Neighboring Seismic Activities in an Area Historical Review (1500_1800). TUBITAK Academic Array, p. 252s.

Angelier, J., 1984. Tectonic analysis of fault slip data sets. J. Geophys. Res.: Solid Earth 89 (B7), 5835–5848, 1978–2012.

Angelier, J., 1990. Inversion of field data in fault tectonics to obtain the regional stress—III. A new rapid direct inversion method by analytical means. Geophys. J. Int. 103 (2), 363–376.

Angelier, J., 1994. Fault slip analysis and paleostress reconstruction. In: Hancock, P.L. (Ed.), Continental Deformation. Pergamon Press, Oxford.

Angus, D.A., Wilson, D.C., Sandvol, E., Ni, J.F., 2006. Lithospheric structure of the Arabian and Eurasian collision zone in eastern Turkey from S-wave receiver functions. Geophys. J. Int. 166, 1335–1346.

Arpat, E., Şaroğlu, F., İz, H., 1977. The earthquake of 1976. Earth and Human 2, 29–41.

Ateş, Ş., Mutlu, G., Özerk, O.Ç., Çiçek, İ., Karakaya Gülmez, F., Bulut Üstün, A., Karabıyıkoğlu, M., Osmançelebioğlu, R., Özata, A., ve Aksoy, A., 2007. Earth Science Data of Van Province, MTA. Department of Geological Studies. Report no.: 10961. 152s (unpublished).

Barka, A.A., Kadinsky-Cade, K., 1988. Strike-slip fault geometry in Turkey and its influence on earthquake activity. Tectonics 7, 663–684.

Bayraktar, A., Altunişik, A.C. ve Pehlivan M., 2013. Performance and damages of reinforced concrete buildings during the October 23 and November 9, 2011 Van, Turkey, earthquakes. Soil Dynam. Earthq. Eng. 53, 49–72.

Berberian, M., 2014. Earthquakes and coseismic surface faulting on the Iranian Plateau; A Historical, social and physical approach. In: In Earth Surface Processes, first ed., vol. 17. Elsevier, Developments, ISBN 978-0-444-63292-0, p. 638p.

Blumenthal, M.M., Van der Kaaden, G., Vlodavetz, V.I., 1964. Catalogue of the active volcanoes of the World including solfatara fields. Part XVII Turkey and the Caucasus. International Association of Volcanology 17, 1–23.

Bozkurt, E., 2001. Neotectonics of Turkey-a synthesis. Geodin. Acta 14 (1–3), 3–30.

Cisternas, A., Philip, H., Bousquet, J.C., Cara, M., Deschamps, A., Dorbath, L., Dorbath, C., Haessler, H., Jimenez, E., Nercessian, A., Rivera, L., Romanowicz, B., Gvishiani, A., Shebalin, N.V., Aptekman, I., Arefiev, S., Borisov, B.A., Gorshkov, A., Graizer, V., Lander, A., Pletnev, K., Rogozhin, A.I., Tatevossian, R., 1989. The Spitak (Armenia) earthquake of 7 December 1988: field observations, seismology and tectonics. Nature 339 (6227), 675–679.

Copley, A., Jackson, J., 2006. Active tectonics of the Turkish-Iranian plateau. Tectonics 25, 1–19.

Cagatay, M.N., Ogretmen, N., Damci, E., Stockhecke, M., Sancar, M., Eris, K.K., Ozeren, S., 2014. lake level and climate records over the last 90 ka from the northern basin of lake van, eastern Turkey. Quat. Sci. Rev. 104, 97–116.

Çukur, D., Krastel, S., Schmincke, H., Sumita, M., Çağatay, N., Meydan, A.F., Damcı, E., Stockhecke, M., 2014. Seismic stratigraphy of lake van, eastern Turkey. Quat. Sci. Rev. 104, 63–84.

Çukur, D., Krastel, S., Schmincke, H., Sumita, M., Tomonaga, Y., Damcı, E., 2013. Drastic lake level changes of Lake Van (eastern Turkey) during the past ca. 600 ka: climatic, volcanic and tectonic control. Am. Geophys. Union.

Çukur, D., Krastel, S., Tomonaga, Y., Schmincke, H., Sumita, M., Meydan, A.F., Çagatay, M.N., Toker, M., Kim, S.P., Kong, G.S., Horozal, S., 2017. Structural characteristics of the Lake Van Basin, eastern Turkey, from high-resolution seismic reflection profiles and multibeam echosounder data: geologic and tectonic implications. Int. J. Earth Sci. 106 (1), 239–253.

Degens, E., Wong, H., Kempe, S., Kurtman, F., 1984. A geological study of lake van, eastern Turkey. Geol. Rundsch. 73 (2), 701–734.

Degens, E.T., Wong, H.K., Kurtman, F., Finckh, P., 1978. Geological development of Lake Van: a summary. The Geology of Lake Van. Miner. Res. Explor. Inst. Turkey (MTA), pp. 134–136.

Delvaux, D., Moeys, R., Stapel, G., Petit, C., Levi, K., Miroshnichenko, A., Ruzhich, V., Sankov, V., 1997. Paleostress reconstructions and geodynamics of the baikal region, central asia. Part II: cenozoic rifting. Tectonophysics 282, 1–38.

Delvaux, D., Sperner, B., 2003. New aspects of tectonic stress inversion with reference to the TENSOR program. Geological Society London Special Publications 212 (1), 75–100.

Dewey, J.F., Hempton, M.R., Kidd, W.S.F., Saroglu, F., Şengor, A.M.C., 1986. Shortening Continental Lithosphere: the Neotectonics of Eastern Anatolia - a Young Collision Zone (Turkey), vol. 19. Geological Society, London, pp. 1–36.

Dewey, J.F., Holdsworth, R.E., Strachan, R.A., 1998. Transpression and Transtension Zones, vol. 135. Geological Society, London, Special Publications, pp. 1–14.

Dhont, D., Chorowicz, J., 2006. Review of the neotectonics of the Eastern Turkish-Armenian Plateau by geomorphic analysis of digital elevation model imagery. Int. J. Earth Sci. 95 (1), 34–49.

Dicle, S., Üner, S., 2017. New active faults on Eurasian-Arabian collision zone: tectonic activity of Özyurt and Gülsünler faults (eastern Anatolian Plateau, Van-Turkey). Geol. Acta: an international earth science journal 15 (2), 107–120.
Djamour, Y., Vernant, P., Nankali, H.R., Tavakoli, F., 2011. NW Iran-eastern Turkey present day kinematics: results from the Iranian permanent GPS network. Earth Planet Sci. Lett. 307, 27–34.
Doğan, B., Karakaş, A., 2013. Geometry of co-seismic surface ruptures and tectonic meaning of the 23 October 2011 M w 7.1 Van earthquake (East Anatolian Region, Turkey). J. Struct. Geol. 46, 99–114.
Ekici, T., Alpaslan, M., Parlak, O., Temel, A., 2007. Geochemistry of the Pliocene basalts erupted along the Malatya-Ovacık fault zone (MOFZ), Eastern Anatolia, Turkey: implications for source characteristics and partial melting processes. Chemie der Erde-Geochemistry 67, 201–212.
Elliott, J.R., Copley, C., Holley, R., Scharer, K., Parsons, B., 2013. The 2011 Mw 7.1 van (eastern Turkey) earthquake. J. Geophys. Res.: Solid Earth 118, 1619–1637.
Emre, O., Duman, T.Y., Ozalp, S., Elmaci, H., 2011. 23 Ekim 2011 Van Earthquake Field Observations and Preliminary Assessment on Resources Fay. General Directorate of Mineral Research and Exploration, Ankara, Turkey.
Emre, Ö., Duman, T.Y., Özalp, S., Olgun, Ş., Elmacı, H., 2013a. Active Fault Map of Turkey Series, Van (NJ 38-5) Layout, Serial No.:52. MTA, Ankara, Turkey.
Emre, Ö., Duman, T.Y., Özalp, S., Elmacı, H., Olgun, Ş., Şaroğlu, F., 2013b. Annotated Active Fault Map of Turkey. Scale 1: 1.250.000. General Directorate of Mineral Exploration and Exploration, Special Publication Series-30, Ankara, Turkey.
EMSC, 2011. European Middle East seismology center. http://www.emsc-csem.org/#2.
Ergin, K., Güçlü, U., Uz, Z., 1967. Turkey and Surrounding Catalog of Earthquakes (MS. 11-1964). Publications of Istanbul, ITU, Faculty of Mines, Institute of Supply Physics.
Eyidoğan, H., Güçlü, U., Utku, Z., Değirmenci, E., 1991. The Largest Earthquake Macroseismic Turkey Directory (1900-1988). Istanbul Technical University, Istanbul, p. 199.
Faccenna, C., Bellier, O., Martinod, J., Piromallo, C., Regard, V., 2006. Slab detachment beneath eastern Anatolia: a possible cause for the formation of the North Anatolian fault. Earth Planet Sci. Lett. 242, 85–97.
Fry, N., 1999. Striated faults: visual appreciation of their constraint on possible paleostress tensors. J. Struct. Geol. 21, 7–21.
Gök, R., Türkelli, N., Sandvol, E., Seber, D., Barazangi, M., 2000. Regional wave propagation in Turkey and surrounding regions. Geophys. Res. Lett. 27, 429–432.
Gök, R., Sandvol, E., Türkelli, N., Seber, D., Barazangi, M., 2003. Sn attenuation in the Anatolian and Iranian plateau and surrounding regions. Geophys. Res. Lett. 30.
Görgün, E., 2013. The 2011 october 23 M-W 7.2 van-ercis, Turkey, earthquake and its aftershocks. Geophys. J. Int. 1052–1067.
Görür, N., Çağatay, N.M., Zabcı, C., Sakinç, M., Akkök, R., Şile, H., Örçen, S., 2015. The late quaternary tectono-stratigraphic evolution of the Lake van, Turkey. Bulletin Of The Mineral Research and Exploration 151, 1–46.
Gürbüz, A., Şaroğlu, F., 2019. Right-lateral strike-slip faulting and related basin formations in the Turkish–Iranian plateau. Developments in Structural Geology and Tectonics 3, 101–130.
Hessami, K., Pantosti, D., Tabassi, H., Shabanian, E., Abbassi, M.R., Feghhi, K., Solaymani, S., 2003. Paleoearthquakes and slip rates of the north Tabriz Fault, NW Iran: preliminary results. Ann. Geophys. 46, 903–916.
Horasan, G., Boztepe-Güney, A., 2007. Observation and analysis of low frequency crustal earthquakes in Lake Van and its vicinity, eastern Turkey. J. Seismol. 11, 1–13.
Innocenti, F., Mazzuoli, R., Pasquare, G., Radicati di Brozolo, F., Villari, L., 1976. Evolution of the volcanism in the area of interaction between the arabian, anatolian and Iranian plates (Lake Van, eastern Turkey). J. Volcanol. Geoth. Res. 1 (2), 103–112.
Innocenti, F., Mazzuoli, R., Pasquare, G., Serri, G., Villari, L., 1980. Geology of the volcanic area north of Lake Van (Turkey). Geol. Rundsch. 69 (1), 292–323.
Jackson, J., 1992. Partitioning of strike-slip and convergent motion between Eurasia and Arabia in eastern Turkey and the Caucasus. J. Geophys. Res. 97, 471–479.
Jolivet, L., Faccenna, C., 2000. Mediterranean extension and the africa-eurasia collision. Tectonics 19 (6), 1095–1106.
Kamar, G., 2018. Palynology of lake arin (eastern Anatolia, Turkey) deposits and its relation with water level change of lake van: preliminary findings. Quat. Int. 468, 83–88.
Karakhanian, A.S., Trifonov, V.G., Philip, H., Avagyan, A., Hessami, K., Jamali, F., Bayraktutan, M.S., Bagdassarian, H., Arakelian, S., Davtian, V., Adilkhanyan, A., 2004. Active faulting and natural hazards in Armenia, eastern Turkey and northwestern Iran. Tectonophysics 380, 189–219.
Karakhanian, A., Vernant, P., Doerflinger, E., Avagyan, A., Philip, H., Arslanyan, R., Champollion, C., Arakelyan, S., Collard, P., Baghdasaryan, H., Peyret, M., Davtyan, V., Calais, E., Masson, F., 2013. GPS constraints on continental deformation in the Armenian region and Lesser Caucasus. Tectonophysics 592, 39–45.
Kempe, S., Khoo, F., Gürleyik, F., 1978. Hydrography of Lake Van and its drainage area. Geology of Lake Van. The Mineral Research and Exploration Institute of Turkey, pp. 30–45.
Kempe, S., Landmann, G., Müller, G., 2002. A floating varve chronology from the last glacial maximum terrace of Lake Van/Turkey. Research in deserts and mountains of Africa and Central Asia 126, 97–114.
Keskin, M., Pearce, J.A., Mitchell, J.G., 1998. Volcano-stratigraphy and geochemistry of collision-related volcanism on the Erzurum-Kars Plateau, northeastern Turkey. J. Volcanol. Geoth. Res. 85, 355–404.
Khorrami, F., Vernant, P., Masson, F., Nilfouroushan, F., Mousavi, Z., Nankali, H., et al., 2019. An up-to-date crustal deformation map of Iran using integratedcampaign-mode and permanent GPS velocities. Geophys. J. Int. 2017, 832–843.
Koçyiğit, A., Yilmaz, A., Adamia, S., Kuloshvili, S., 2001. Neotectonic of East Anatolian plateau (Turkey) and lesser Caucasus: implication for transition from thrusting to strikeslip faulting. Geodin. Acta 14 (1–3), 177–195.
Koçyiğit, A., 2013. New field and seismic data about the intraplate strike-slip deformation in Van region, East Anatolian plateau, E. Turkey. J. Asian Earth Sci. 62, 586–605.
KOERI, 2011-2012. Boğaziçi university kandilli observatory and earthquake Research institute. Recent earthquakes. http://www.koeri.boun.edu.tr/scripts//lst5.asp.
Kuzucuoğlu, C., Christol, A., Mouralis, D., Doğu, A.F., Akköprü, E., Fort, M., Brunstein, D., Zorer, H., Fontugne, M., Karabıyıkoğlu, M., 2010. formation of the upper Pleistocene terraces of lake van (Turkey). J. Quat. Sci. 25 (7), 1124–1137.
Lahn, E., 1946. Note on van zone ground shaking (July-December 1945). MTA journal 1/35, 126–132.
Lebedev, V., Sharkov, E., Keskin, M., Oyan, V., 2010. Geochronology of late Cenozoic volcanism in the area of Van Lake, Turkey: an example of development dynamics for magmatic processes. Dokl. Earth Sci. 1031–1037.
Lisiecki, L.E., Raymo, M.E., 2005. A Pliocene-Pleistocene stack of 57 globally distributed benthic d18O records. Paleoceanography 20.
Litt, T., Krastel, S., Sturm, M., Kipfer, R., Örçen, S., Heumann, G., Franz, S.O., Ülgen, U. B., Niessen, F., 2009. 'PALEOVAN', international continental scientific drilling program (ICDP): site survey results and perspectives. Quat. Sci. Rev. 28, 1555–1567.
Mackenzie, D., Elliott, J.R., Altunel, E., Walker, R.T., Kurban, Y.C., Schwenninger, J.-L., Parsıns, B., 2016. Seismotectonics and rupture process of the MW 7.1 2011 Van reverse-faulting earthquake, Eastern Turkey, and implications for hazard in regions of distributed shortening. Geophysical Journal International Advance Access 1–56.
McClusky, S., Balassanian, S., Barka, A., Demir, C., Ergintav, S., Georgiev, I., Gürkan, O., Hamburger, M., Hurst, K., Kahle, H., et al., 2000. Global Positioning System constraints on plate kinematics and dynamics in the eastern Mediterranean and Caucasus. J. Geophys. Res. 105, 5695–5719.
McKenzie, D., 1972. Active tectonics of the Mediterranean Region. Geophys. J. Roy. Astr. S. 109–185.
Michael, A.J., 1984. Determination of stress from slip data: faults and folds. J. Geophys. Res. 89, 11 517–11 526.
Mouralis, D., Kuzucuoğlu, C., Scaillet, S., Doğu, A.F., Christol, A., Akköprü, E., et al., 2010. Les pyroclastites du sudouest du lac de Van (Anatolie orientale, Turquie): implications sur la palèo-hydrographie règionale. Quaternaire 21, 417–433.
Mutlu, S., Üner, T., 2019. Petrological properties of ultramaphic rocks and associated mafic dykes observed in savatlı-özalp ophiolite (Van-Eastern Anatolia). Journal of Çukurova University Faculty of Engineering and Architecture 34 (1), 115–128.
Notsu, K., Fujitani, T., Ui, T., Matsuda, J., Ercan, T., 1995. Geochemical features of collision-related volcanic rocks in central and eastern Anatolia, Turkey. J. Volcanol. Geoth. Res. 64, 171–191.
Okay, A.I., Zattin, M., Cavazza, W., 2010. Apatite fission-track data for the Miocene Arabia- Eurasia collision. Geology 38, 35–38.
Özacar, A.A., Gilbert, H., Zandt, G., 2008. Upper mantle discontinuity structure beneath East Anatolian Plateau (Turkey) from receiver functions. Earth Planet Sci. Lett. 269, 426–434.
Özacar, A.A., Zandt, G., Gilbert, H., Beck, S.L., 2010. Seismic images of crustal variations beneath the East Anatolian Plateau (Turkey) from teleseismic receiver functions, 340, 485–496.
Özalp, S., Aydemir, B.S., Olgun, Ş., Şimşek, B., Elmacı, H., Evren, E., Emre, Ö., Aydın, M. B., Kurtuluş, O., Öcal, F., Can, A.Z., Yanmaz, M.N., Apa, R., Duman, T.Y., 2016. Tectonic Deformations in the Quaternary Deposits of the Lake Van (Edremit Bay), Eastern Anatolia, Turkey, vol. 153. Bulletin Of The Mineral Research and Exploration.
Özkaymak, Ç., Sözbılır, H., Bozkurt, E., Dırık, K., Topal, T., Alan, H., Çağlan, D., 2011. Seismic geomorphology of 23 october 2011 based-van earthquake and its relationship with active tectonic structures in eastern Anatolia. Journal of Geological Engineering 35 (2), 175–199.
Philip, H., Avagyan, A., Karakhanian, A., Ritz, J.F., Rebai, S., 2001. Estimating slip rates and recurrence intervals for strong earthquakes along an intracontinental fault: example of the Pambak-Sevan-Sunik fault (Armenia). Tectonophysics 343, 205–232.
Pearce, J.A., Bender, J.F., De Long, S.E., Kidd, W.S.F., Low, P.J., Güner, Y., Şaroglu, F., Yılmaz, Y., Moorbath, S., Mitchell, J.G., 1990. Genesis of collision volcanism in eastern Anatolia, Turkey. J. Volcanol. Geoth. Res. 44, 189–229.
Pınar, N., Lahn, E., 1952. Earthquake in Turkey Annotated Catalog. Ministry of Public Works, Construction and Development Works Directorate, Ankara. No. 6.
Rebai, S., Philip, H., Dorbath, L., Borissoff, B., Haessler, H., Cisternas, A., 1993. Active tectonics in the lesser Caucasus: coexistence of compressive and extensional structures. Tectonics 12 (5), 1089–1114.
Reches, Z., 1987. Determination of the tectonic stress tensor from slip along faults that obey Coumomb yield condition. Tectonics 6, 849–861.
Reilinger, R., McClusky, S., Vernant, P., Lawrence, S., Ergintav, S., Cakmak, R., Ozener, H., Kadirov, F., Guliev, I., Stepanyan, R., Nadariya, M., Hahubia, G., Mahmoud, S., Sakr, K., ArRajehi, A., Paradissis, D., Al-Aydrus, A., Prilepin, M., Guseva, T., Evren, E., Dmitrotsa, A., Filikov, S.V., Gomez, F., Al-Ghazzi, R., Karam, G., 2006. GPS constraints on continental deformation in the Africa-Arabia-Eurasia continental collision zone and implications for the dynamics of plate interactions. J. Geophys. Res.: Solid Earth 111.
REDPUMA, 2003. Swiss Seismology Center web page. http://seismo.ethz.ch/moment_tensor.
Rizza, M., Vernant, P., Ritz, J.F., Peyret, M., Nankali, H., Nazari, H., Djamour, Y., Salamati, R., Tavakoli, F., Chery, J., Mahan, S.A., Masson, F., 2013. Morphotectonic and geodetic evidence for a constant slip-rate over the last 45 kyr along the Tabriz fault (Iran). Geophys. J. Int. 193, 1083–1094, 2013.

Sandvol, E., Seber, D., Calvert, A., Barazangi, M., 1998. Grid search modeling of receiver functions: implications for crustal structure in the Middle East and North Africa. Journal of Geophysical Research B: Solid Earth 103, 26899–26917.
Sağlam-Selçuk, A., Erturaç, M.K., Nomade, S., 2016. Geology of the Caldiran Fault, Eastern Turkey: age, slip rate and implications on the characteristic slip behaviour. Tectonophysics 680, 155–173.
Selçuk, L., Selçuk, A.S., Beyaz, T., 2010. Probabilistic seismic hazard assessment forLake Van basin, Turkey. Nat. Hazards 54, 949e965.
Şengör, A.M.C., Yılmaz, Y., 1983. Tethyan evolution of Turkey: a plate tectonic approach. Tectonophysics 75 (3–4), 181–190, 193-199,203-241.
Solaymani Azad, S., Philip, H., Dominguez, S., Hessami, K., Shahpasandzadeh, M., Foroutan, M., Lamothe, M., 2015. Paleoseismological and morphological evidence of slip rate variations along the North Tabriz fault (NW Iran). Tectonophysics 640–641. https://doi.org/10.1016/j.tecto.2014.11.010, 20–38.
Soysal, H., Sipahioğlu, S., Koçak, D., Altınok, Y., 1981. Historical Earthquake Catalog of Turkey and the Environment (2100 BC-AD 1900). TUBİTAK Project (TBAG), Ankara, Turkey.
Stockhecke, M., Kwiecien, O., Vigliotti, L., Anselmetti, F.S., Beer, J., Çağatay, M.N., Channell, J.E.T., Kipfer, R., Lachner, J., Litt, T., Pickarski, N., Sturm, M., 2014a. Chronostratigraphy of the 600.000 year old continental record of Lake Van (Turkey). Quat. Sci. Rev. 104, 8–17.
Stockhecke, M., Sturm, M., Brunner, I., Schmincke, H.U., Sumita, M., Kwiecien, O., Çukur, D., Anselmetti, F.S., 2014b. Sedimentary evolution and environmental history of Lake Van (Turkey) over the past 600.000 years. Sedimentology 61 (6), 1830–1831.
Şaroğlu, F., 1986. Geological and Structural Evolution of Eastern Anatolia in the Neotectonic Period. PhD thesis. Istanbul University, Institute of Science, Geological Engineering Department (unpublished).
Şaroğlu, F., Yılmaz, Y., 1986. Geological evolution and watershed models in the neotectonic period in Eastern Anatolia. Mineral Research and Exploration Magazine 107, 73–94.
Şaroğlu, F., Yılmaz, G., Erdoğan, R., 1984. Geological Feature of the Horasan – Narman Earthquake and the Necessity of Earthquake-Related Studies in Eastern Anatolia, the 1st National Earthquake Symposium of Northeast Anatolia. Atatürk University, Erzurum, pp. 349–360.
Şaroğlu, F., Emre, Ö., Boray, A., 1987. Turkey's Active Faults and Earthquakes. the MTA report, Ankara, Turkey.
Şaroğlu, F., Emre, Ö., Kuşçu, İ., 1992. Active Fault Map of Turkey. General Directorate of Mineral Research and Exploration, Ankara Turkey.
Şengör, A.M.C., Görür, N., Şaroğlu, F., 1985. Strike-slip faulting and related basin formation in zonesof tectonic escape: Turkey as a case study. Soc. Econ. Paleontol. Mineral. Spec. Publ. 37, 227–264.
Şengör, A.M.C., Kidd, W.S.F., 1979. Post-collisional tectonics of the Turkish-Iranian plateau and a comparison with Tibet. Tectonophysics 55 (3–4), 361–376.
Şengör, A., Özeren, S., Genç, T., Zor, E., 2003. East Anatolian high plateau as a mantle-supported, north-south shortened domal structure. Geophys. Res. Lett. 30 (24).
Şengör, A.M.C., Özeren, M.S., Keskin, M., Sakınç, M., Özbakır, A.D., Kayan, İ., 2008. Eastern Turkish high plateau as a small Turkic-type orogen: implications for postcollisional crust-forming processes in Turkic-type orogens. Earth Sci. Rev. 90, 1–48.
Tan, O., Tapirdamaz, M.C., Yörük, A., 2008. The earthquake catalogues for Turkey. Turk. J. Earth Sci. 17 (2), 405–418.
Tan, O., 2004. Welding Mechanism Properties and Tearing Processes of Caucasia, Eastern Anatolia and Northwest Iran Earthquakes. Ph.D. Thesis. ITU Institute of Science, Istanbul (unpublished).
Taymaz, T., 1990. Earthquake Source Parameters in the Eastern Mediterranean Region [Ph.D. Thesis]: Darwin College. University of Cambridge, Cambridge.
Toker, Ö., Şengör, A.M.C., Demirel Schluter, F., Demirbag, E., Cukur, D., Imren, C., Niessen, F., PaleoVan-Working Group, 2017. The structural elements and tectonics of the Lake Van basin (Eastern Anatolia) from multi-channel seismic reflection profiles. J. Afr. Earth Sci. 129, 165–178.
Toksöz, M.N., Arpat, E., Şaroglu, F., 1977. East Anatolian earthquake of 24 november 1976. Nature 270, 423–425.
Toksöz, M.N., Guenette, M., Gülen, L., Keough, G., Pulli, J.J., Sav, H., Olguner, A., 1983. "Narman–Horasan depreminin kaynak mekanizması". Yeryuvarı ve İnsan 8, 47–52.
Trifonov, V.G., Karakhanian, A.S., Berberian, M., Ivanova, T.P., Kazmin, V.G., Kopp, M. L., Kozhurin, A.I., Kuloshvili, S.I., Lukina, N.V., Mahmud, S.M., Vostrikov, G.A., Swedan, A., Abdeen, M., 1996. Active faults of the Arabian plate bounds, Caucasus and Middle East. J. Earthquake Prediction Research 5, 363–374.
TUBITAK, 2011. The Scientific and Technological Research Council of Turkey. Marmara Research Center. http://www.mam.gov.tr/.
Türkelli, N., Horasan, G., Kuleli, H., Reiter, D., 1996. Preliminary results of velocity distribution study in eastern Turkey. Eos, Transaction American Geophysical 77, 477.
USGS, 2011. United States geological survey. http://www.usgs.gov.
Üner, S., Yeşilova, Ç., Yakupoğlu, T., Üner, T., 2010. Deformation structures (seismites) caused by earthquakes in unconsolidated sediments: Van Lake Basin, Eastern Anatolia. Earth sciences 31 (1), 53–66.
Üner, S., Alırız, M.G., Özsayın, E., Sağlam Selçuk, A., Karabıyıkoğlu, M., 2017. Earthquake induced sedimentary structures (Seismites): geoconservation and promotion as geological heritage (Lake Van-Turkey). Geoheritage 9 (2), 133–139.
Üner, S., Özsayın, E., Sağlam Selçuk, A., 2019. Seismites as an indicator for determination of earthquake recurrence interval: a case study from Erciş Fault (Eastern Anatolia-Turkey). Tectonophysics 766, 167–178.
Üner, S., 2003. Sedimentology of Plio-Quaternary terrestrial sediments east of Lake Van (Beyüzümü-Göllü). Van Yüzüncü Yıl University.
Üner, T., 2019. Listwaenitization and Enrichment of Precious Metals in the Hydrothermal Mineralization Zones of Serpentinites in Sugeçer-Van (Eastern Anatolia, Turkey). Geochemistry: Exploration, Environment, Analysis, geochem 2018-087.
Wong, H., Finckh, P., 1978. Shallow structures in lake van. In: Degens, E.T., Kurtman, F. (Eds.), The the Geology Lake Van. MTA, pp. 20–29.
Yilmaz, Y., Şaroğlu, F., Güner, Y., 1987. Initiation of the neomagmatism in east Anatolia. Tectonophysics 134 (1–3), 177–199.
Zor, E., 2008. Tomographic evidence of slab detachment beneath eastern Turkey and the Caucasus. Geophys. J. Int. 175, 1273–1282.
Zor, E., Sandvol, E., Gürbüz, C., Türkelli, N., Seber, D., Barazangi, M., 2003. The crustal structure of the East Anatolian plateau (Turkey) from receiver functions. Geophys. Res. Lett. 30, 7-1/7-4.